GeoExpert ag

swiss*nuclear*: PEGASOS Refinement Project:
SP2 – Ground Motion Characterization

Contract no. PMT-VT-1032

Seismic Shear Wave Velocity Determination and Hybrid Seismic Survey at the SED-Station SKEH (Kerns OW)

Date of Field Data Acquisition 22nd March 2009

Report

Client

swiss*nuclear*
Project PRP
Frohburgstrasse 17
4601 Olten

Contractor

GeoExpert ag
Seismic Prospecting
Ifangstrasse 12b
P.O. Box 451
8603 Schwerzenbach

8603 Schwerzenbach, 26th May 2009

INDEX

1 INTRODUCTION

1.1 Survey objectives

The seismic survey's main task is to provide information about the distribution function of the shear wave velocities in the depth interval of the uppermost 30 m along a 100 m long seismic profile.

Additionally, the following objectives are to be met:

- the mapping of the topography of the rock face, i.e. the thickness of the Quaternary deposits;
- the determination of the thickness of the weathered zone and its degree of decompaction at the bedrock surface;
- a general view of geological structures.

1.2 The choice of the appropriate surveying methods

Several methods are available for deriving the s-wave velocity distribution in the subsurface at any given position:

- in-situ measurement by down-hole or crosshole seismic surveying;
- shear-wave refraction tomography profiling;
- dispersion analysis of surface waves (MASW; **M**ultiple channel **A**nalysis of **S**urface **W**aves)

The surveys are to be carried out at, or as close as possible near some 20 SED earth quake monitoring stations in Switzerland. Ideally, the surveys are to be conducted on two orthogonal profiles in order to derive at their point of intersection a robust 1D s-wave velocity distribution function by correlation. To this end, the methods of MASW and shear-wave refraction tomography profiling are to be combined.

The results are to include the following fundamental parameters $v_{s,5}$, $v_{s,10}$, $v_{s,20}$, $v_{s,30}$, $v_{s,40}$, $v_{s,50}$, $v_{s,100}$ are to be calculated, also an error estimation of all values.

The data acquired for the MASW method are to be subjected to complementary **p-wave hybrid seismic data processing** in order to image the geological structures.

2 FIELD DATA ACQUISITION PARTICULARS

2.1 Time Schedule

Date	*Time*	*Activities / remarks*
18.12.2008	0900	arrival from Schwerzenbach at site
	0900 - 0915	site inspection
	0915 - 1025	lay-out of recording spread profile 1 (p-wave)
		lay-out of recording spread profile 1 (s-wave)
	1025 - 1105	data recording of profile 1 (p-wave)
	1120 - 1215	data recording of profile 1 (s-wave)
	1215 - 1410	retrieval of the recording spread
		lay-out of recording spread profile 2 (p-wave)
		lay-out of recording spread profile 2 (p-wave)
	1410 - 1435	data recording of profile 2 (p-wave)
	1445 - 1525	data recording of profile 2 (s-wave)
	1250 - 1330	retrieval of the recording spread
	1330	departure from site

2.2 Summary of Data Acquisition Parameters

Compressional Wave Data Acquisition

# of active channels	96
geophone type	4.5 Hz natural frequency, vertical velocimeter
receiver station spacing	1.0 m
# of geophones/station	1
source point spacing	2.0 m to 3.0 m
source type	vertical hammer (6 kg) striking on a horizontal metal plate
sampling rate	500 µs
recording time	2048 ms
field filters	0.5 Hz LC, anti-alias
# of field records	47 (line 09SN_13SKEH-P1) and 44 (line 09SN_13SKEH-P2)

Fig. 2.1: Seismic data acquisition: lay-out of geophone and jumper cables along the house wall. The seismic monitoring station is located in a chamber below the bicycle kid.

Shear Wave Data Acquisition

# of active channels	48
geophone type	10 Hz natural frequency, horizontal velocimeter
receiver station spacing	2.0 m
# of geophones/station	1
source point spacing	4.0 m
source type	horizontal hammer (6 kg) striking horizontally at a metal-plated wooden beam anchored to the ground by means of 20 cm long spikes
sampling rate	500 µs
recording time	256 ms
field filters	2 Hz LC, anti-alias
# of field records	52 at 26 positions (line 09SN_13SKEH-S1) and 50 at 25 positions (line 09SN_13SKEH-S2)

Fig. 2.2: Seismic shear wave data acquisition: striking the metal-plated wooden beam with a 8 kg hammer in both directions (from left and right).

2.3 Composition of Seismic Field Crew

Personnel

Keller Lorenz	dipl. Natw. ETH, party chief, geophysicist
Fiseli Jochen	Dipl.-Geologe, Uni Freiburg i. Br., seismic observer, geophysicist
Martin Dieter	Dipl.-Geologe, Uni Freiburg i. Br., spread lay-out, handle of seismic source

Equipment

96	vertical geophones 4.5 Hz
48	horizontal geophones 10 Hz
6	seismic cables
1	seismic acquisition system Summit Compact, 96 channels
1	laptop computer for data acquisition
3	walkie-talkies
1	hammer 6 kg
1	steel plate
1	metal-plated wooden beam
1	van (FIAT Ducato 4x4)

2.4 Location

The seismic monitoring station SKEH is situated on a relatively flat ridge of Cretaceous and Tertiary sediments central Switzerland, canton of Obwalden. The sediments are composed of massive sandstones and limestones. A quaternary alluvial fan of unknown thickness covers the solid rock.

Fig. 2.3: The red cross marks the location of the seismic monitoring station SKEH on cretaceous sediments. (map: geodata @ swisstopo).

2.5 Recording Conditions and Line Setup

The data acquisition was done on a cold, windy day. The strong wind and air traffic noise temporarily reduce the signal quality significantly.

In general, the data quality obtained under the prevailing conditions is to be rated as fair to good.

The Fig. 2.4 shows the situation an SED station SKEH.

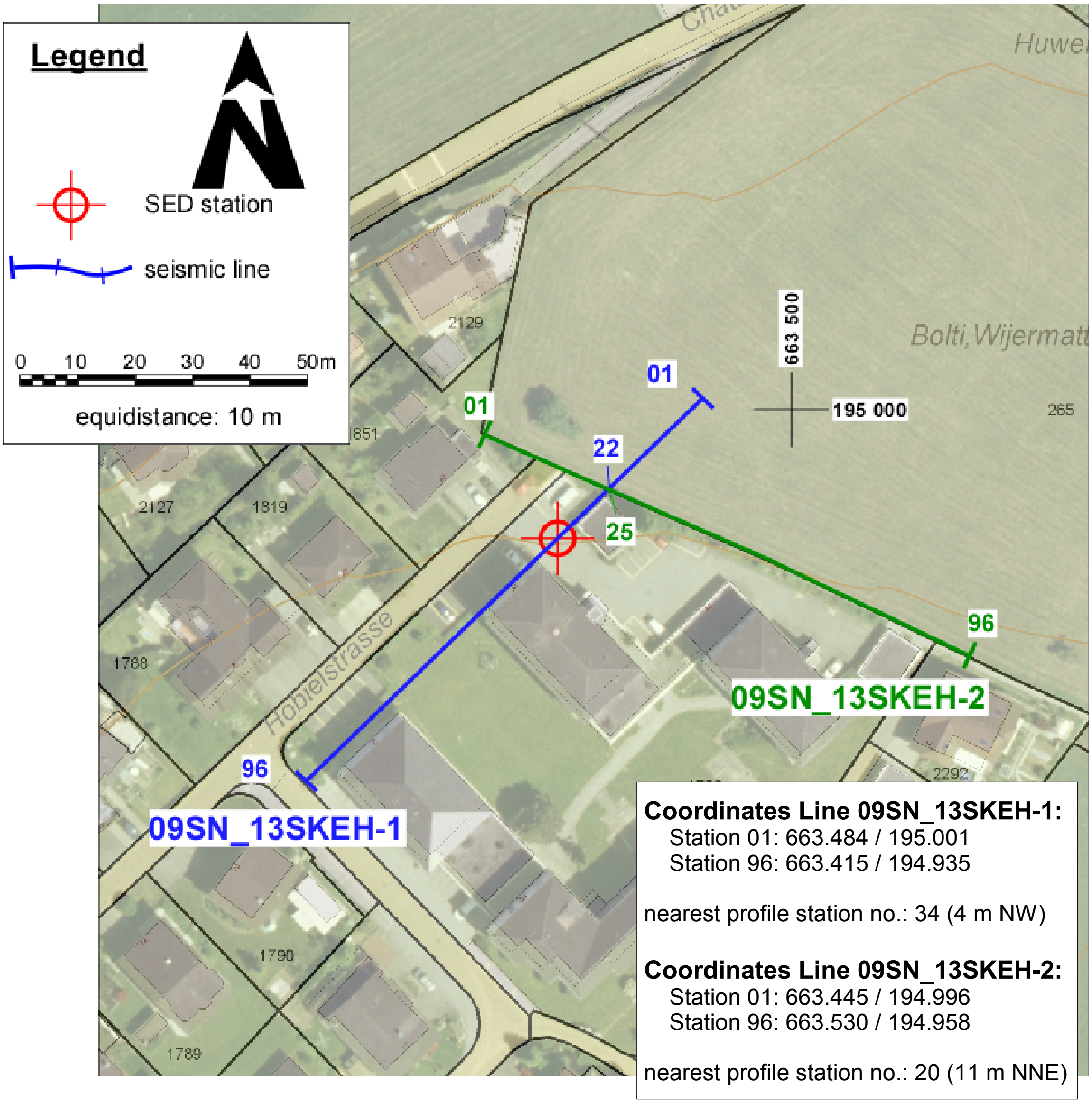

Fig. 2.3: Situation map with the trace of seismic profile 09SN_13SKEH-1 and -2. (background map and aerial photo: © GIS OW)

3 SEISMIC DATA PROCESSING AND IMAGING OF THE RESULTS

3.1 General Remarks

- For the shear and compressional wave refraction seismic evaluation the package **RAYFRACT** by Intelligent Resources Ltd., Vancouver CAN, was used. The system features the technique of diving wave tomography (www.rayfract.com).
- The system **SPW** (**S**eismic **P**rocessing **W**orkshop) of Parallel Geoscience Corporation, Austin US-TX, was used for reflection seismic data processing (www.parallelgeo.com).
- Data processing of surface waves (MASW processing) was conducted with the software package **SurfSeis** V2.0 of Kansas Geological Survey in Lawrence US-KS.

A detailed description of the various surveying methods will be included in the general summary report.

3.2 Shear Wave Refraction Tomography

3.2.1 Reformatting and field geometry assignment

After reformatting the field data into the Rayfract format the field geometry is applied.

3.2.2 First break time picking

At each shot position, two seismic records were acquired in both activation directions. These two records are displayed superimposed with different colors on each other in Fig 3.2a together with the manually determined first arrival time picks.

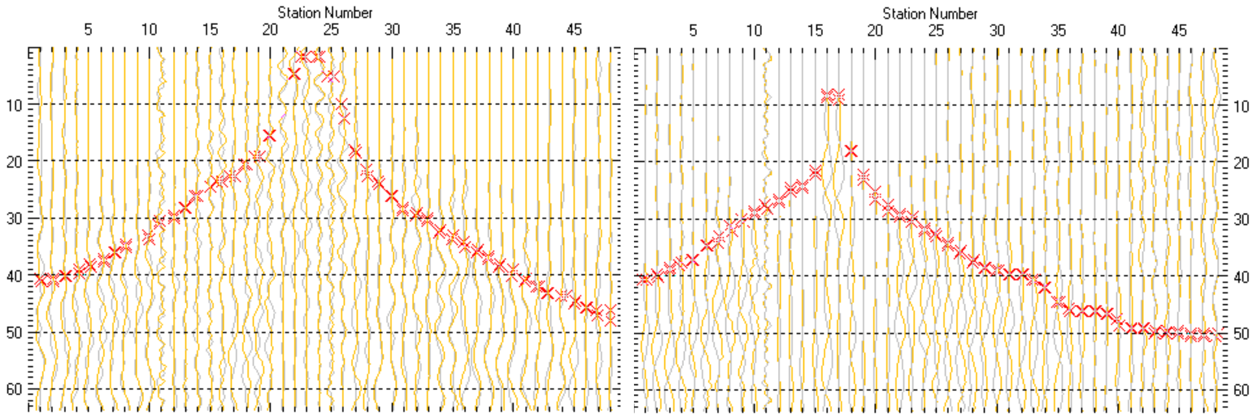

*Fig. 3.2a: High quality dual field record from line 09SN_13SKEH-S1 (left) and -S2 (right).showing at each station the s-wave traces with opposing polarities in different colors. The manually picked s-wave refraction arrivals at each station are marked with an **x**. The station spacing is 2 m, profile station number 00 = profile meter 0; profile station number 48 = profile meter 96.*

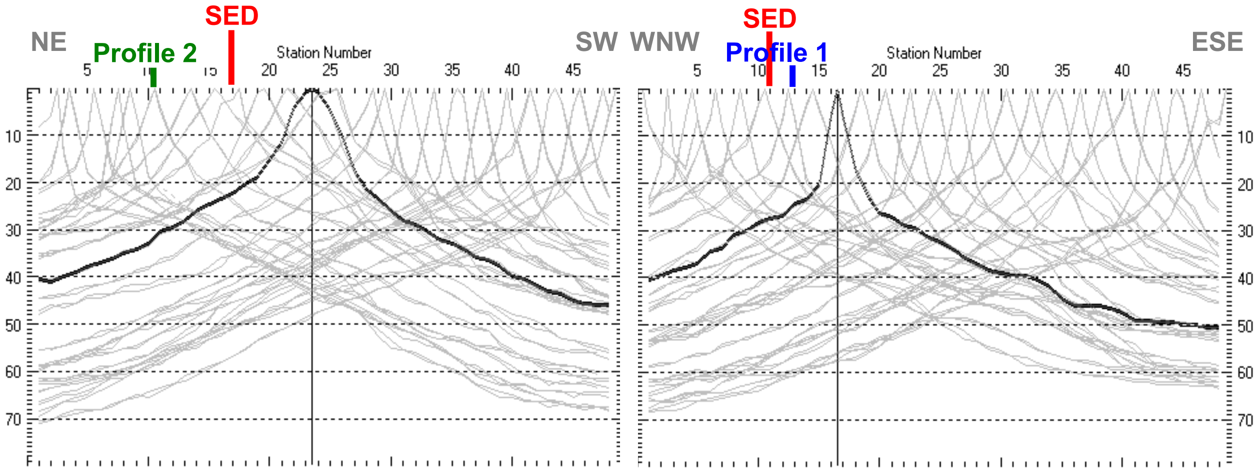

Fig. 3.2b: Curves of s-wave first break time picks from line 09SN_13SKEH-S1 (left) and -S2 (right).

3.2.3 Analytical Determination of Refraction Velocities

An initial 1D-velocity function (averaged 1D velocity-depth profiles derived by the Delta-t-V method, see Tab. 3.2a) is determined in the 3-dimensional time-offset-CMP-domain from all first break arrival time curves in the 3-dimensional time-offset-CMP-domain (see. Fig. 3.2c).

Depth [m]	Vs [m/s]
0.0	441
0.4	460
0.7	481
1.1	504
1.8	612
2.5	739
3.4	904
4.6	1113
6.4	1315
8.7	1474
11.7	1644
15.8	1695
21.3	1978
28.4	2504
37.9	3322

Depth [m]	Vs [m/s]
0.0	230
0.4	265
0.7	299
1.1	333
1.8	458
2.5	609
3.4	810
4.7	1080
6.5	1272
8.8	1542
11.8	1860
16.0	2247
21.5	2489
28.7	3351
38.4	4652

Tab. 3.2a: Initial 1D s-wave velocity function derived from real data from line 09SN_13SKEH-S1 (mean values between profile meters 30 and 60) and from line 09SN_13SKEH-S2 (mean values between profile meters 30 and 60).

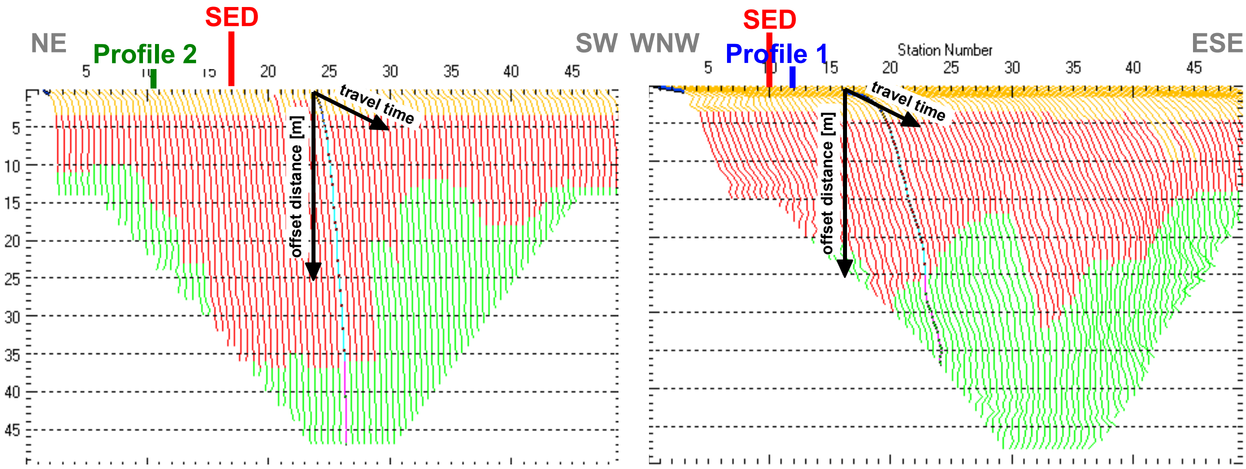

Fig. 3.2c: 3-dimensional distance-travel time diagrams from line 09SN_13SKEH-S1 (left) and -S2 (right) at the mid-points between source points and receiver stations are instrumental when using the analytical CMP derivation of the initial velocity field.
The horizontal axes are the along the CMP positions and the travel time respectively, the vertical axis denotes the offset distance between source and receiver positions. The colors represent different velocity layers. The station spacing is 2 m, profile station number 00 = profile meter 0; profile station number 48 = profile meter 96. The colors represent different velocity layers.

3.2.4 Tomographic inversion of the velocity gradient field by iterative modeling

The velocity field is iteratively refined by the subsequent Wavepath Eikonal Traveltime (WET) tomographic inversion process. The inversion results are portrayed in Fig. 3.2d as a gridded velocity contour section and in Fig. 3.2e as a ray path density section.

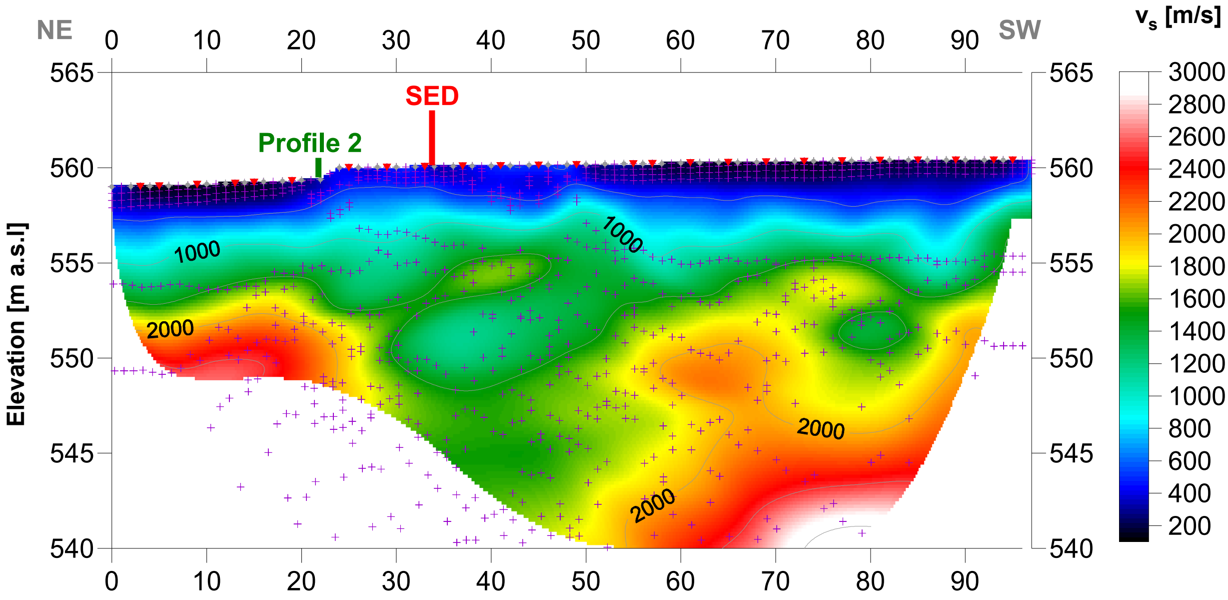

Fig. 3.2d: Shear wave velocity field of the line 09SN_13SKEH-S1. Red/white colors denote solid rock, blue/black colors point to unconsolidated sediments and soil.
Vertical axis: elevation [m a.s.l]; horizontal axis: profile meter; color encoded scale: v_s [m/s]; vertical exaggeration: 2:1; gray diamonds: receiver positions; red triangles: source positions; magenta crosses: positions of determined velocity values. The station spacing is 2 m, profile meter 0 = profile station number 00, profile meter 96 = profile station number 48.

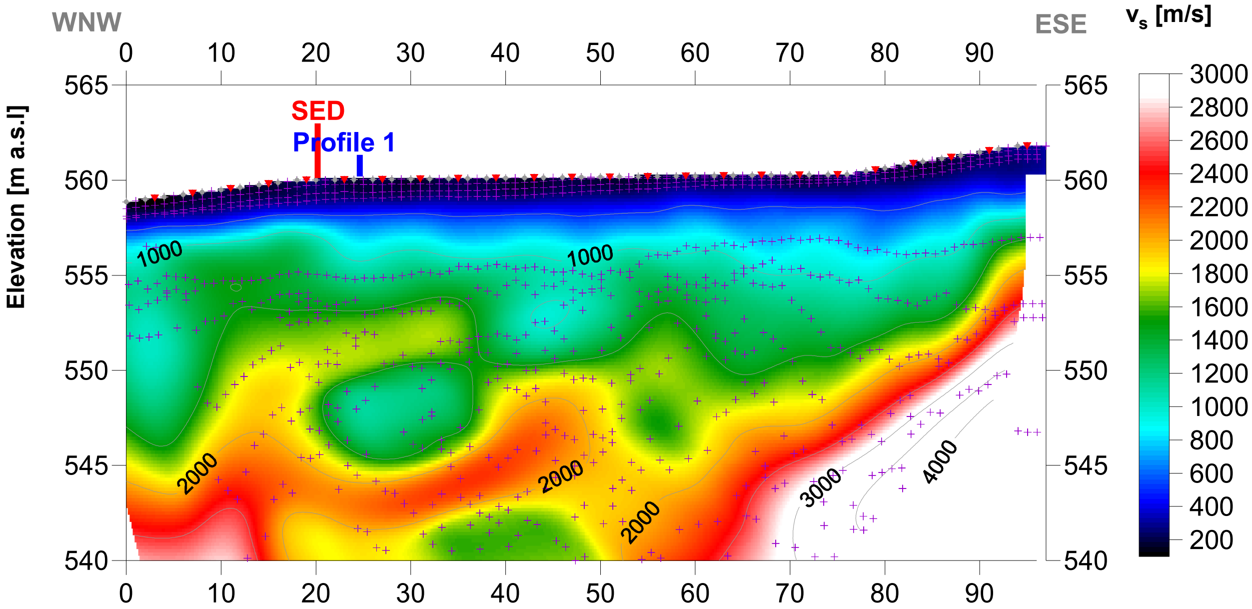

Fig. 3.2e: Shear wave velocity field of the line 09SN_13SKEH-S2. Red/white colors denote solid rock, blue/black colors point to unconsolidated sediments and soil. Vertical axis: elevation [m a.s.l]; horizontal axis: profile meter; color encoded scale: v_s [m/s]; vertical exaggeration: 2:1; gray diamonds: receiver positions; red triangles: source positions; magenta crosses: positions of determined velocity values. The station spacing is 2 m, profile meter 0 = profile station number 00, profile meter 96 = profile station number 48.

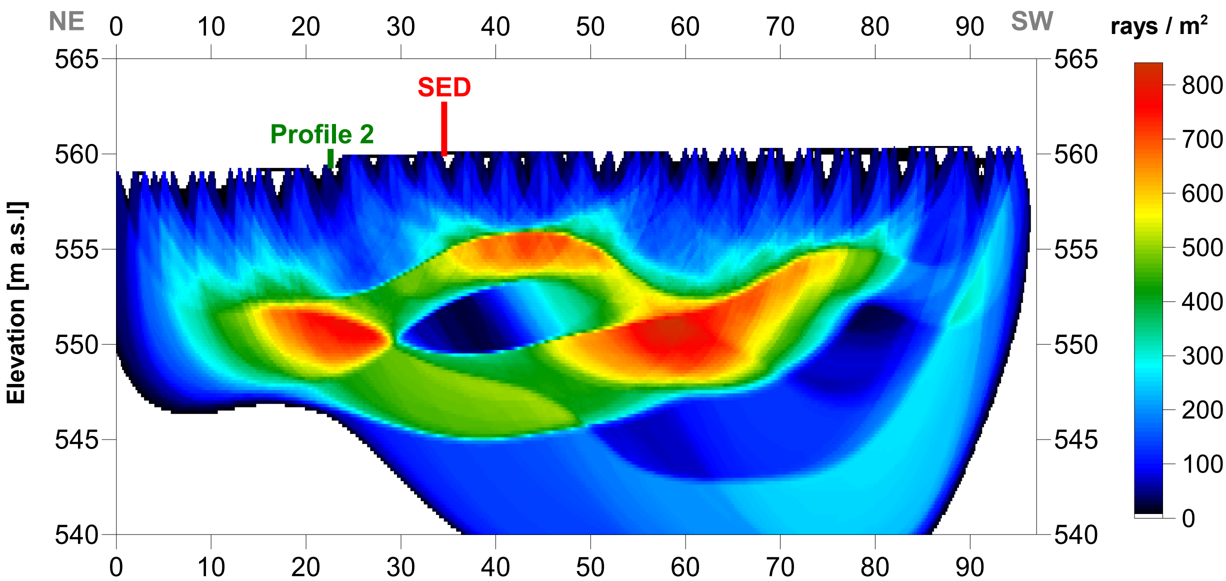

Fig. 3.2f: Shear wave ray path density along the seismic line 09SN_13SEKH-S1. Red/white colors indicate high velocity contrasts (usually at the bedrock surface), blue/black colors denote low coverage areas. Vertical axis: elevation [m a.s.l]; horizontal axis: profile meter; color encoded scale: ray paths per m²; vertical exaggeration: 2:1. The station spacing is 2 m, profile meter 0 = profile station 00, profile meter 96 = profile station 48.

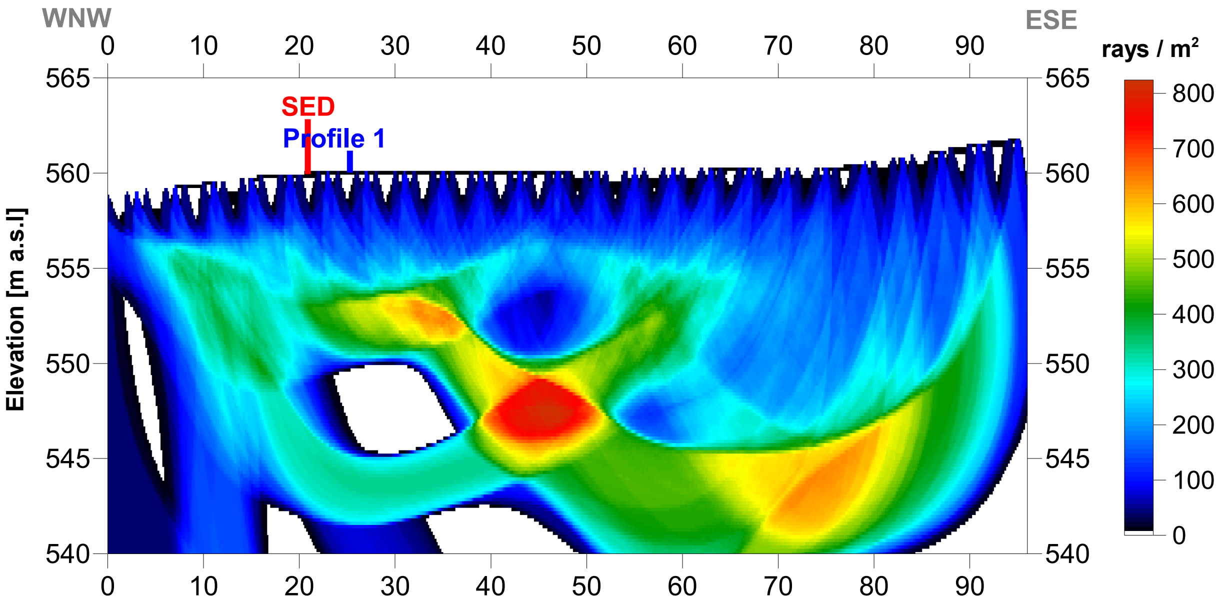

Fig. 3.2f: Shear wave ray path density along the seismic line 09SN_13SKEH-S2. Red/white colors indicate high velocity contrasts (usually at the bedrock surface), blue/black colors denote low coverage areas. Vertical axis: elevation [m a.s.l]; horizontal axis: profile meter; color encoded scale: ray paths per m²; vertical exaggeration: 2:1. The station spacing is 2 m, profile meter 0 = profile station 00, profile meter 96 = profile station 48.

Depth [m]	Vs [m/s]
0.0	372
1.4	535
2.8	928
4.3	1255
5.7	1434
7.1	1424
8.5	1395
9.9	1495
11.3	1649
12.8	1649
14.2	1624
15.6	1650
16.8	1747
18.3	1890
19.7	2061

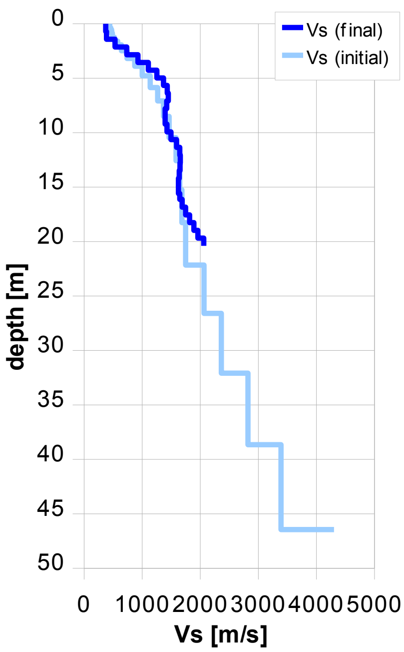

Tab. 3.2b: Final 1D s-wave velocity model derived from real data from line 09SN_13SKEH-S1 (horizontal average of all values) for the profile segment (between profile meters 30 and 60) with a geological setting resembling the one at the SED station. The calculated values of the initial 1D s-wave velocity model are given in Tab. 3.2a.

Depth [m]	Vs [m/s]
0.0	184
1.8	518
3.6	932
5.4	1229
7.2	1324
9.0	1468
10.8	1649
12.6	1739
14.4	1940
16.2	2064
17.8	1834
19.6	1807
21.4	1926
23.1	2091
24.9	2361
26.7	2433
28.5	2430
30.0	2549

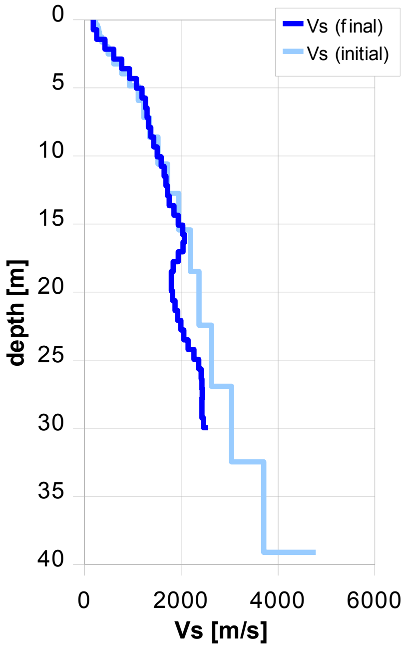

Tab. 3.2c: Final 1D s-wave velocity model derived from real data from line 09SN_13SKEH-S2 (horizontal average of all values) for the profile segment (between profile meters 30 and 60) with a geological setting resembling the one at the SED station. The calculated values of the initial 1D s-wave velocity model are given in Tab. 3.2a.

Due to lack of sufficient data quality on MASW analyses, we derived the $v_{s,5}$, $v_{s,10}$, $v_{s,20}$, $v_{s,30}$ scalar values from seismic refraction tomographic analyses:

	Vs,5	Vs,10	Vs,20	Vs,30
Vs1	620	862	1137	
Vs2	420	638	941	1164
MEAN	520	750	1039	1164

Tab. 3.2d: The average shear wave velocities within the depth intervals from surface down to 5 m, etc. … to 50 m, calculated for the line segment with a subjectively most similar geology to the SED station (profile station 30 to 60 on both lines).

3.3 MASW Processing

3.3.1 Reformatting and field geometry assignment

The data preparation steps for the dispersion analysis include

- the assignment of the field acquisition geometry
- the selection of suitable offset ranges (=arrays) between 10 m and 50 m for dispersion, and the splitting of the field records in forward and reverse shooting direction data sets
- the reformatting of the data into the specific KGS format

X - - ... - - o-o-o-...-o-o-o (forward shooting or so-called PLUS direction)
respectively
o-o-o-...-o-o-o - - ... - - X (reverse shooting or so-called MINUS direction).

where **X** = shot position
o = receiver station
- = 1.0 m offset

The active array used at SED-station SKEH are the receiver station in the shot offset range between 10 and 50 m.

3.3.2 Calculating the dispersion image (overtone)

The result of dispersion analysis is the color encoded acoustic energy distribution in the phase velocity - frequency plane (see Fig. 3.3a and b).

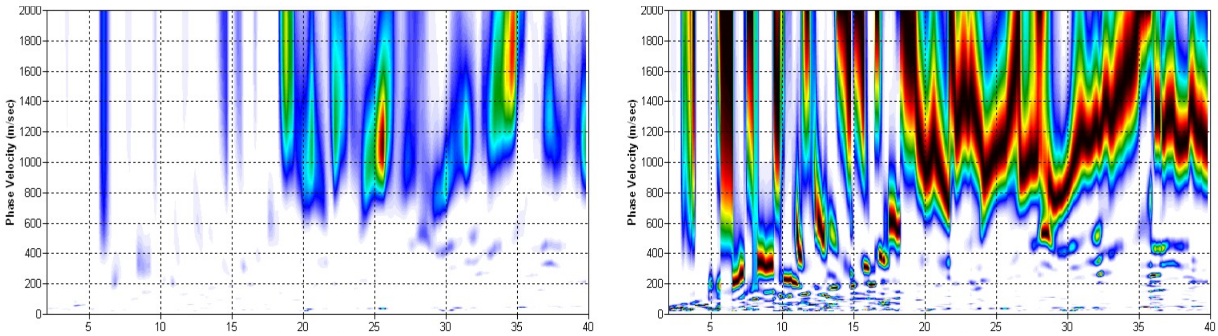

*Fig. 3.3a: Dispersion images of a record (40 m array, mid station 37) of the MASW dataset of line 09SN_13SKEH-M1 (plus direction, light). For the determination of the dispersion curves, the records are **normalized** (right).*
Horizontal axis: frequency from 5 to 40 Hz; vertical axis: phase velocity from 0 to 2000 m/s; color code: colors from white (no energy) to blue - green - yellow - red - black point to increasing energy amplitude values.

3.3.3 Analysis of the dispersion image

In the dispersion graphs as calculated in section 3.3.2 above, the curves joining the amplitude peaks of the fundamental modes are determined either by subjective inspection or in a semi-automated manner. On datasets with poorly defined amplitude peaks or with a highly irregular alignment of the peaks, the danger of obtaining improbable or wrong results is real and can only be mitigated by the processing experience and the a-priori knowledge of the geological setting by the geophysicist responsible for the data evaluation.

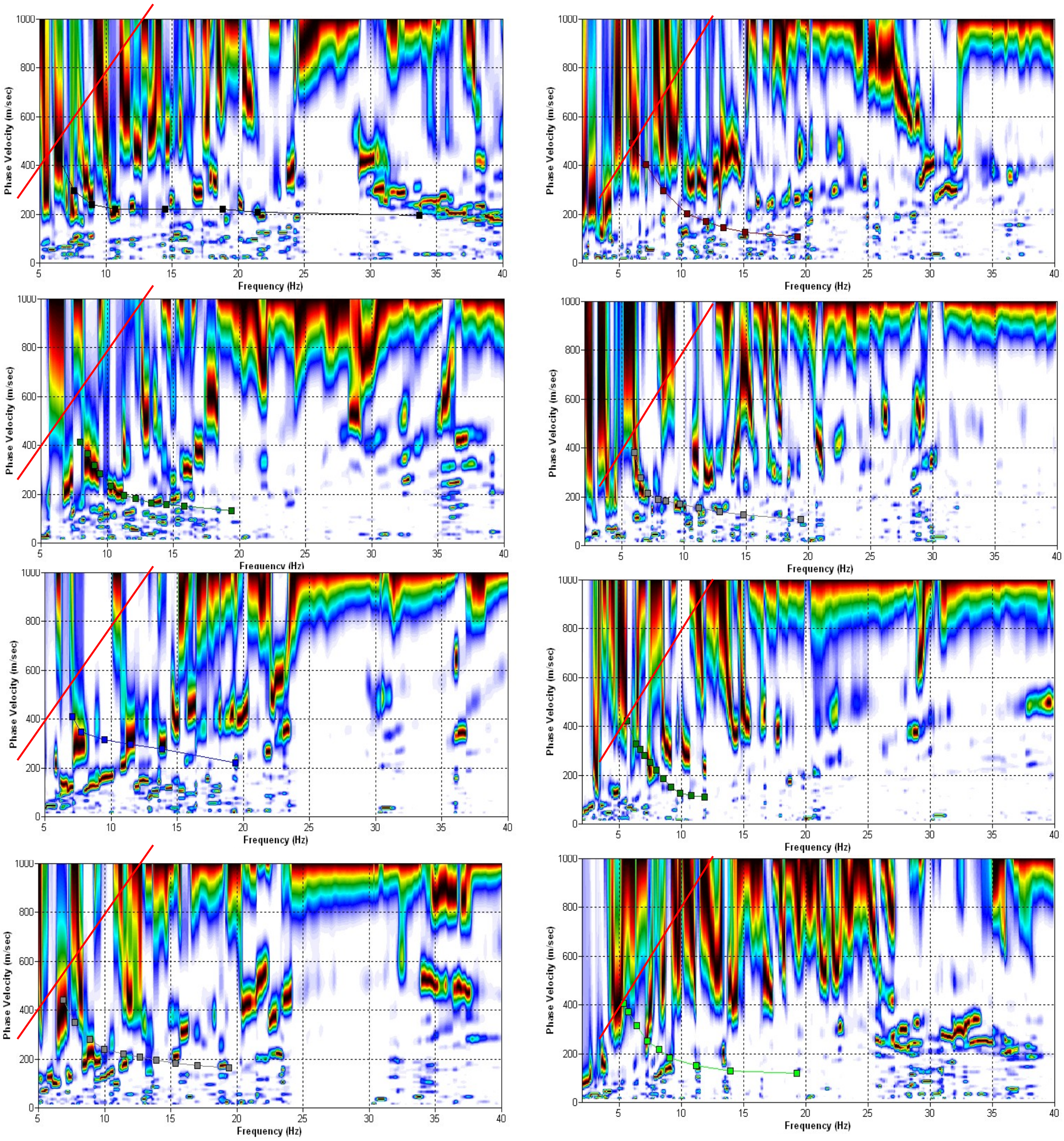

Fig. 3.3b: The manually picked dispersion images used for the derivation of the shear wave velocity section on line 09SN_13SKEH-M1. The dispersion curves (squares) are determined by linking the peaks of high energy. Note that 'higher modes' may at times produce higher energy peaks than the fundamental mode required for the analysis.
Note: The dispersion images are normalized.
dotted fine line: signal-noise ratio for the designated f-v_{ph} – value.
red line: high resolution beam-forming curve for v_{max}.
1st row: left: station 31 @ PLUS direction; right: station 35 @ MINUS direction
2nd row: left: station 37 @ PLUS direction; right: station 38 @ MINUS direction
3rd row: left: station 45 @ PLUS direction; right: station 47 @ MINUS direction
4th row: left: station 50 @ PLUS direction; right: station 56 @ MINUS direction

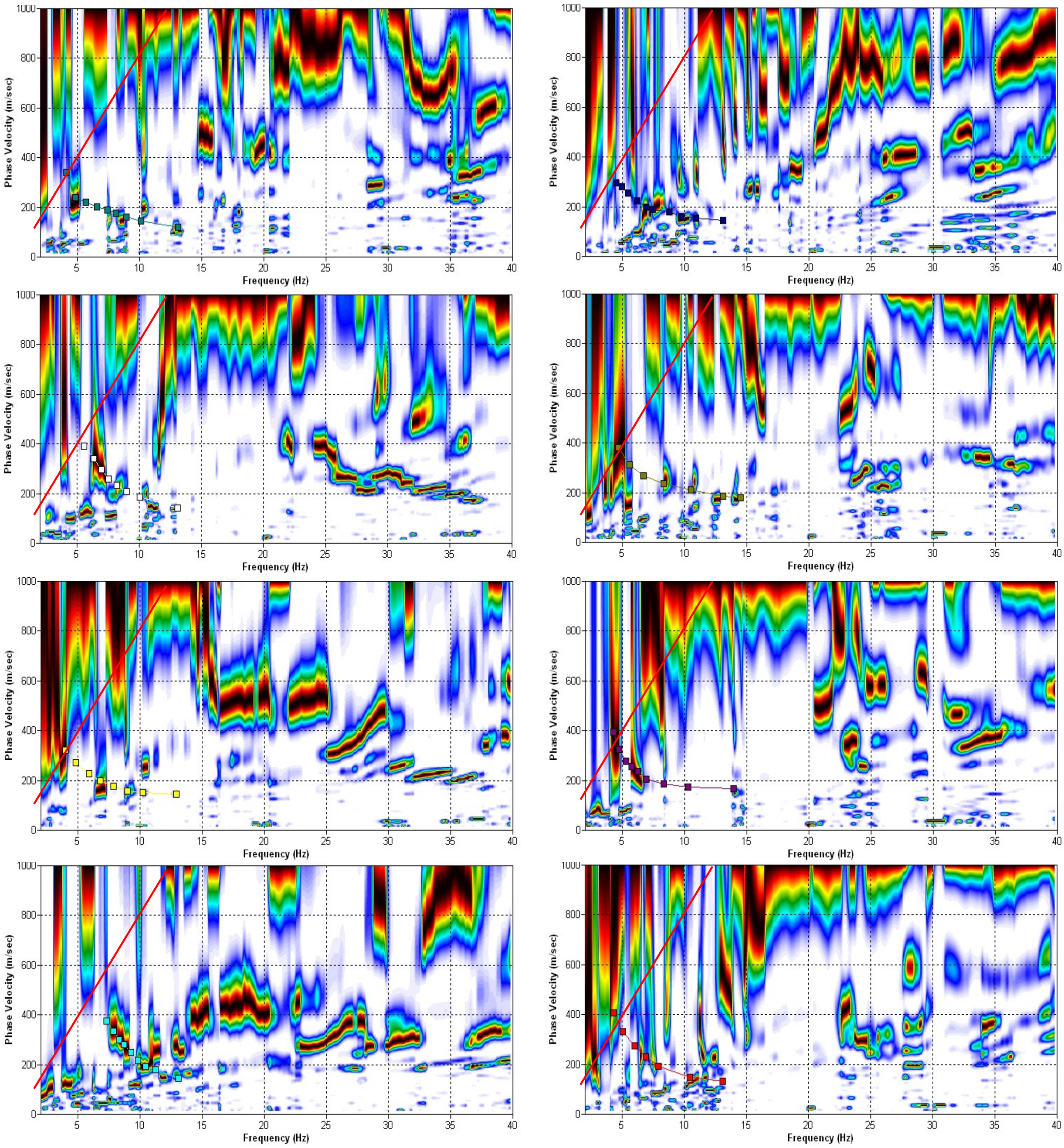

Fig. 3.3c: The manually picked dispersion images used for the derivation of the shear wave velocity section on line 09SN_13SKEH-M2. The dispersion curves (squares) are determined by linking the peaks of high energy. Note that 'higher modes' may at times produce higher energy peaks than the fundamental mode required for the analysis.
Note: The dispersion images are normalized.
dotted fine line: signal-noise ratio for the designated f-v_{ph} – value.
red line: high resolution beam-forming curve for v_{max}.
1st row: left: station 29 @ PLUS direction; right: station 35 @ MINUS direction
2nd row: left: station 41 @ PLUS direction; right: station 38 @ MINUS direction
3rd row: left: station 50 @ PLUS direction; right: station 47 @ MINUS direction
4th row: left: station 59 @ PLUS direction; right: station 56 @ MINUS direction

3.3.4 Inversion of dispersion curves resulting in a 1D shear wave velocity distribution

Inversion of the extracted dispersion curves was performed using the algorithm described by Xia et al. (1999).

The inversion process is started by setting the maximum depth (z_{max}) to be in the order of 30% of the largest wavelength for an initial model consisting of 10 layers of increasing thicknesses. For all 10 layers the Poisson's ratio is assumed to be 0.4 and the rock/soil density to be 2.0 g/cm^3. The inversion process is concluded either after twelve iterations or when the convergence condition of a RMS-error of less than 3 m/s (phase velocity) is met.

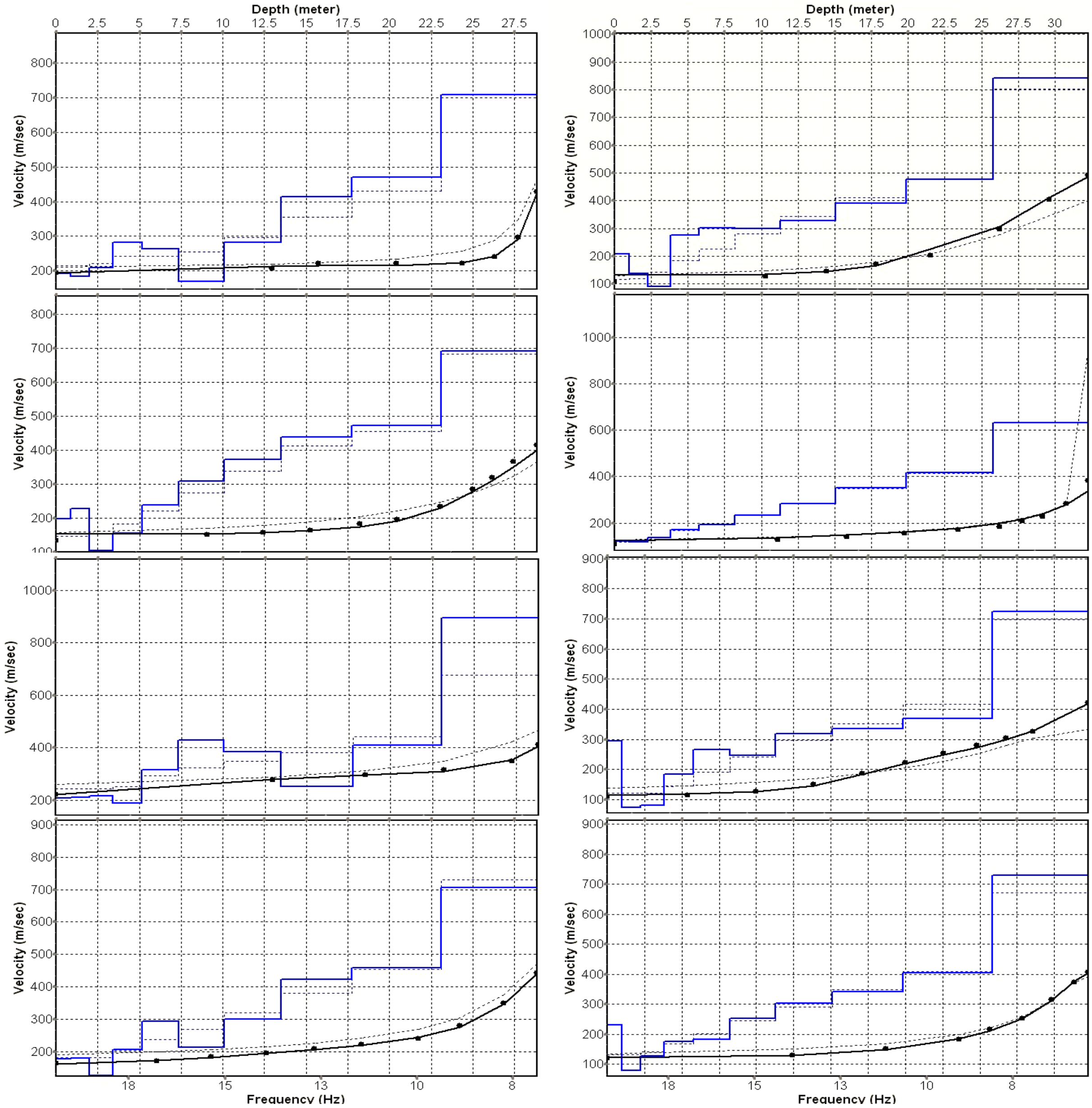

Fig. 3.3d: Inversion results of dispersion curves from dataset at line 09SN_13SKEH-M1.
***brown**: Inversion of dispersion curve (dots) resp. of the modeled dispersion curve (dotted line: initial model; continuous line: end model). Horizontal axis: frequency Hz, vertical axis: v_s.*
***blue**: 10-layer-model (dotted: initial model, continuous line: final model). Horizontal axis: depth, vertical axis: phase velocity resp. v_s).*
1st row: left: station 31 @ PLUS direction; right: station 35 @ MINUS direction
2nd row: left: station 37 @ PLUS direction; right: station 38 @ MINUS direction
3rd row: left: station 45 @ PLUS direction; right: station 47 @ MINUS direction
4th row: left: station 50 @ PLUS direction; right: station 56 @ MINUS direction

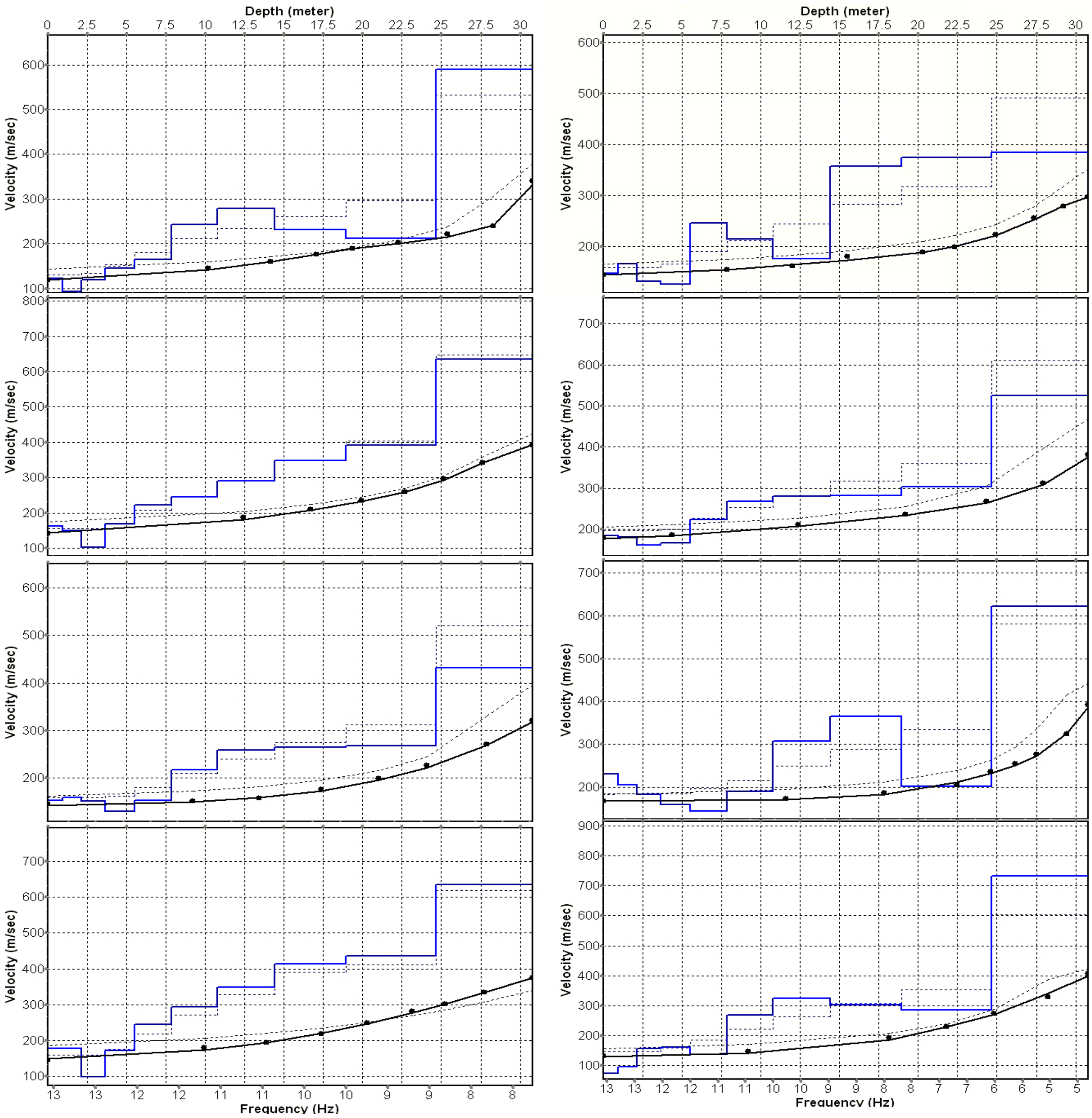

Fig. 3.3e: Inversion results of dispersion curves from dataset at line 09SN_13SKEH-M2.
***brown**: Inversion of dispersion curve (dots) resp. of the modeled dispersion curve (dotted line: initial model; continuous line: end model). Horizontal axis: frequency Hz, vertical axis: v_s.*
***blue**: 10-layer-model (dotted: initial model, continuous line: final model). Horizontal axis: depth, vertical axis: phase velocity resp. v_S).*
1st row: left: station 29 @ PLUS direction; right: station 35 @ MINUS direction
2nd row: left: station 41 @ PLUS direction; right: station 38 @ MINUS direction
3rd row: left: station 50 @ PLUS direction; right: station 47 @ MINUS direction
4th row: left: station 59 @ PLUS direction; right: station 56 @ MINUS direction

Dispersion analyses of records with longer receiver arrays should – by theory – increase the investigation depth. At SKEH, with both lines and both directions, MASW processing with the maximal array length of 94 m doesn't improve the results (Fig. 3.3f and 3.3g).

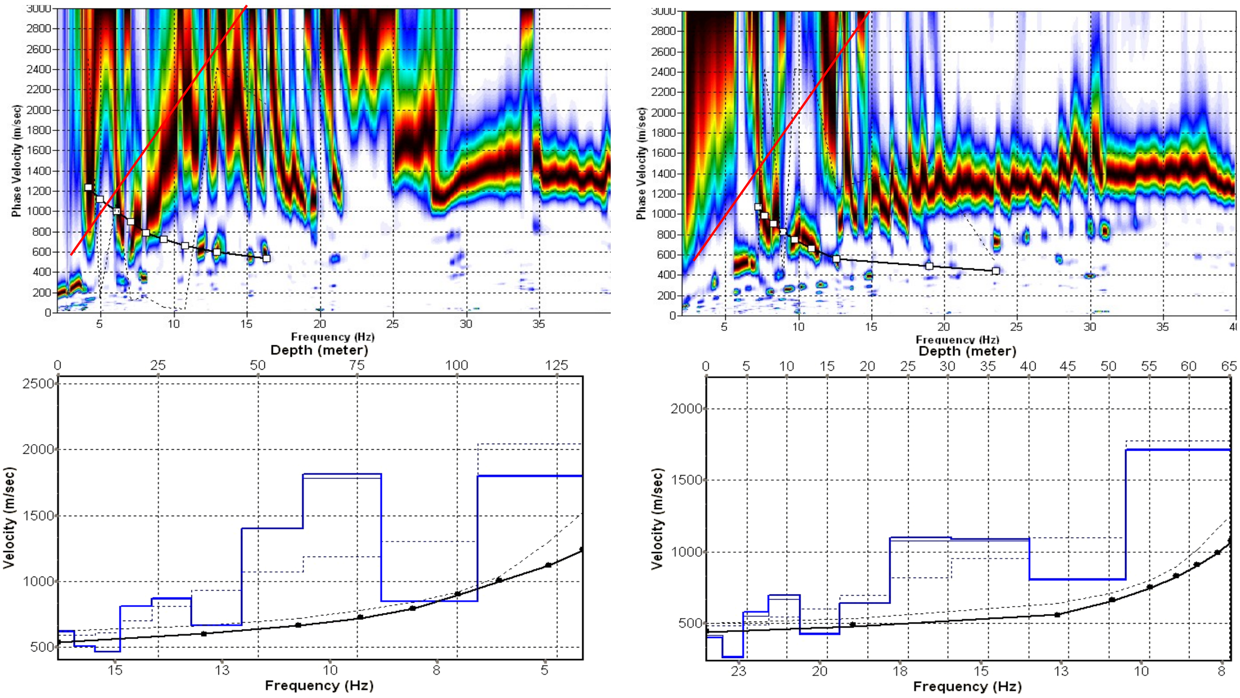

Fig. 3.3f: Top: dispersion images of over-all arrays (10...104 m offset) from line 09SN_13SKEH-M1 in PLUS (left) and MINUS (right) direction; dotted fine line: signal-noise ratio for the designated f-v_{ph}-value. Red line: high resolution beam-forming curve for v_{max}.
Note: The dispersion images are normalized.
*Below: The two respective inversion results; **brown**: inversion of dispersion curve; **blue**: 10-layer-model. Horizontal axis: depth, vertical axis: phase velocity resp. v_s.*

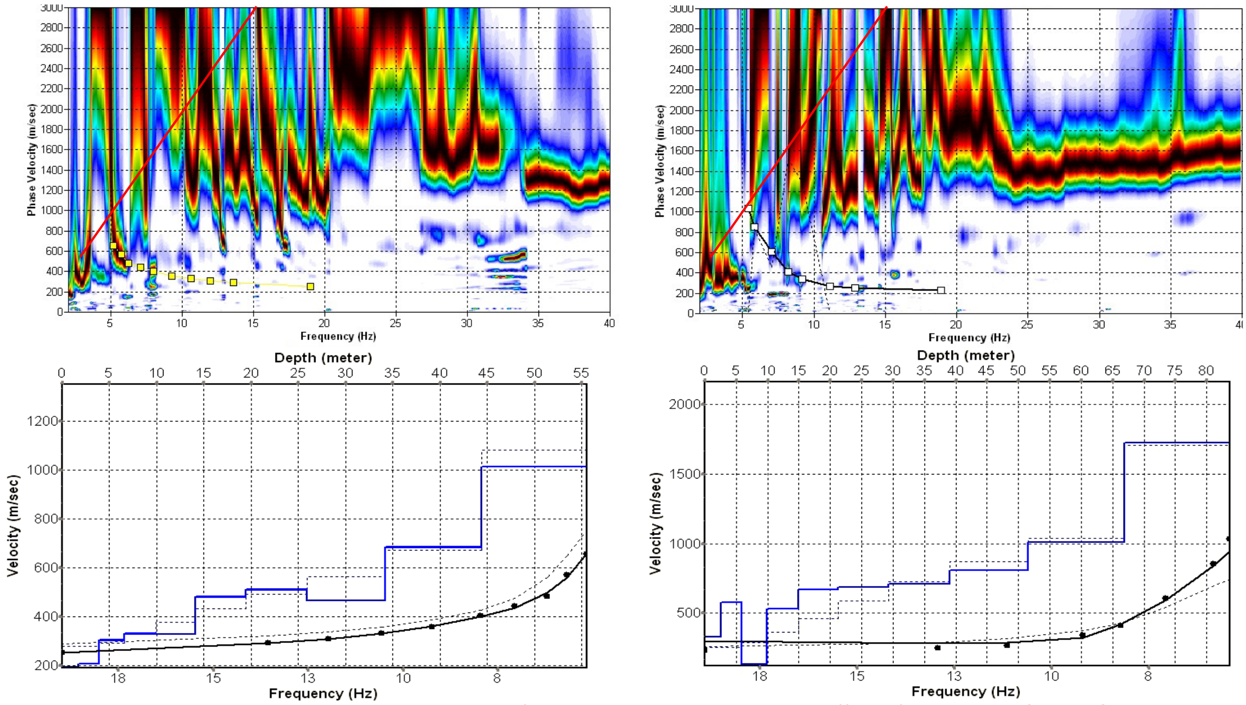

Fig. 3.3g: Top: dispersion images of over-all arrays (10...104 m offset) from line 09SN_13SKEH-M2 in PLUS (left) and MINUS (right) direction; dotted fine line: signal-noise ratio for the designated f-v_{ph} – value. Red line: high resolution beam-forming curve for v_{max}.
Note: The dispersion images are normalized.
*Below: The two respective inversion results; **brown**: inversion of dispersion curve; **blue**: 10-layer-model. Horizontal axis: depth, vertical axis: phase velocity resp. v_s.*

3.3.5 Gridding and plotting of 2D v_s-velocity field

By assembling the 1D v_S - depth functions from all stations the final 2D v_S-field is derived using a Kriging gridding procedure as portrayed in Fig. 3.3h and 3.3i below:

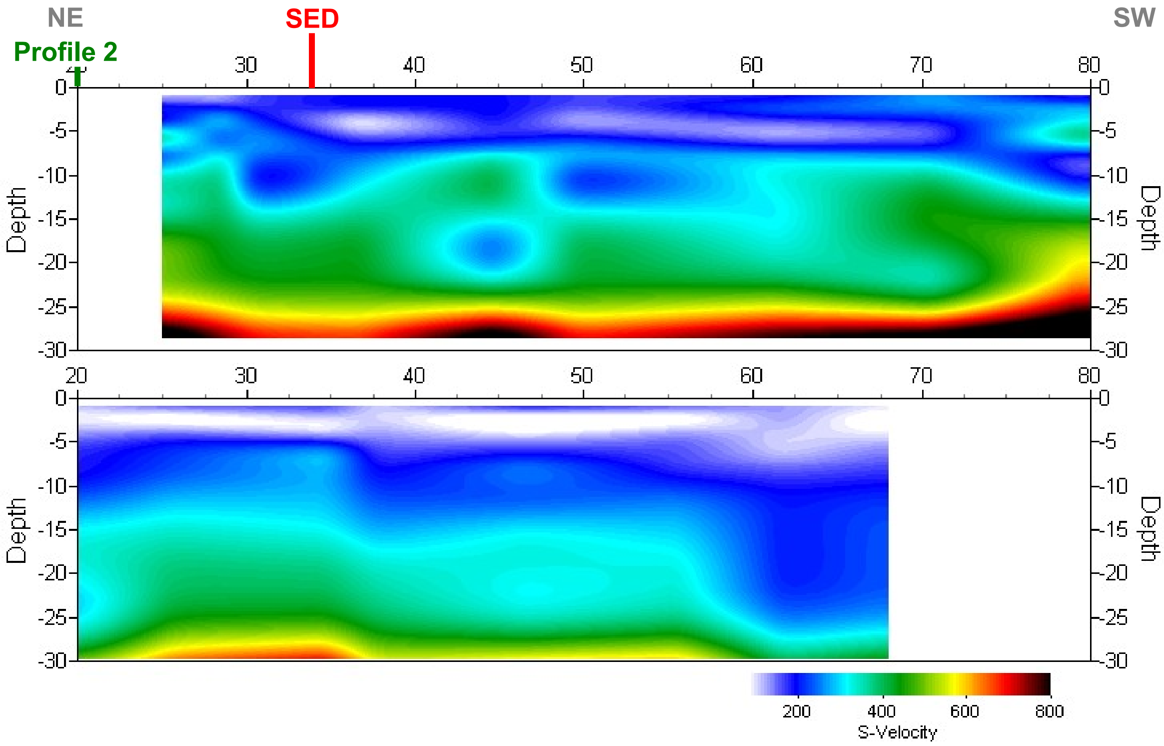

Fig. 3.3h: PLUS- (above) and MINUS- (below)-MASW-processed shear wave velocity fields from line 09SN_13SKEH-M1. Station spacing is 1 m.

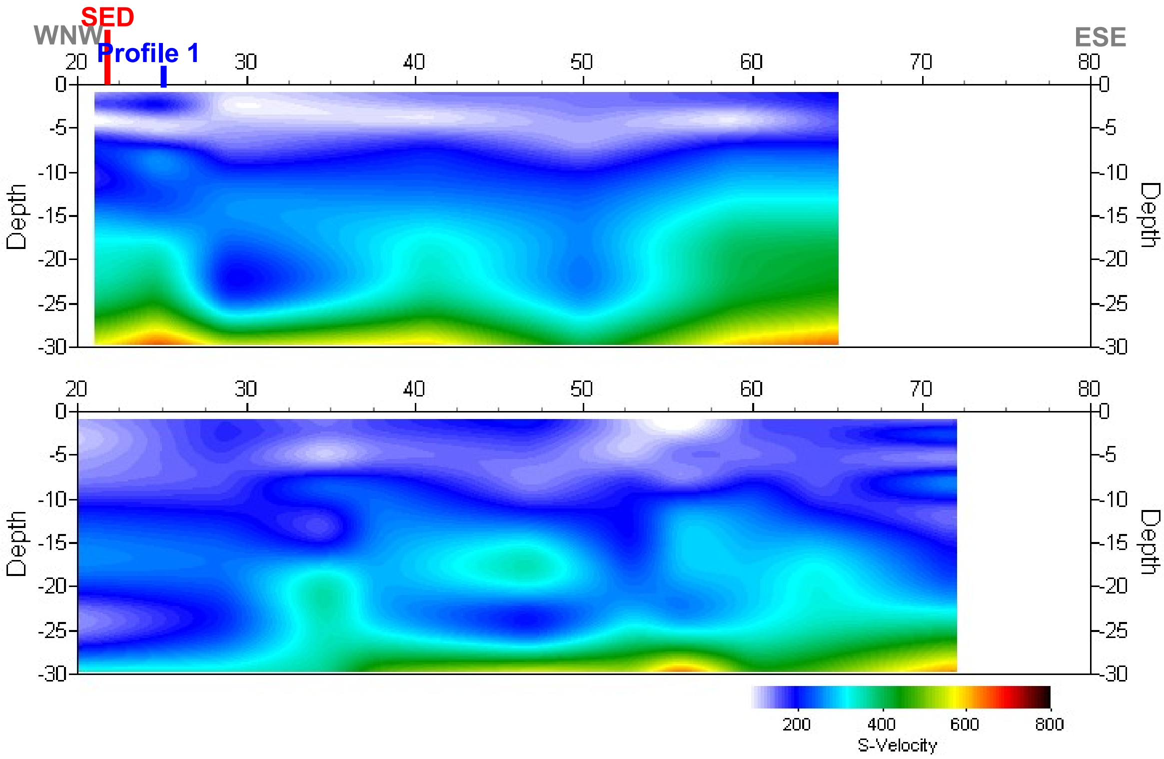

Fig. 3.3i: PLUS- (above) and MINUS- (below)-MASW-processed shear wave velocity fields from line 09SN_13SKEH-M2. Station spacing is 1 m.

3.3.6 Calculation of the average shear wave velocity

In order to calculate a representative shear wave velocity-depth function from line 09SN_13SKEH-M1 at the SED station, all computed 1D-v_S-depth functions between seismic profile station no. 30 and 60 – that are four profiles in each direction – are averaged (non-weighted mean values). The v_S-depth-function is shown in Tab. 3.3a.

Depth [m]	Vs+ [m/s]	Vs- [m/s]	Vs [m/s]
0.9	213	194	204
2.1	102	200	151
3.6	109	163	136
5.5	201	208	205
7.8	236	277	256
10.7	257	279	268
14.3	309	335	322
18.8	355	381	368
24.5	416	452	434
30.6	732	749	740

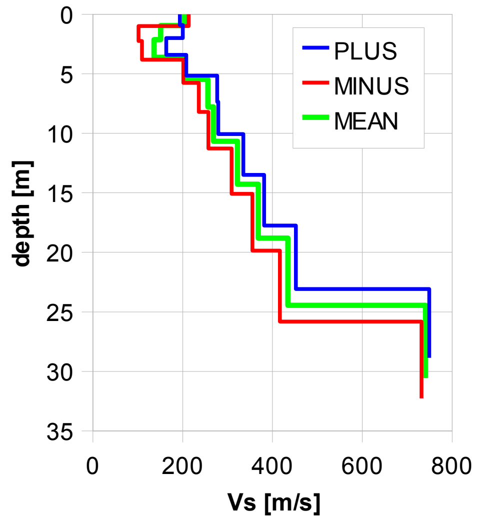

Tab. 3.3a: Averaged vs - depth function from line 09SN_13SKEH-M1 at the SED station SKEH. Blue line: MASW-'PLUS' processing, red line: MASW-'MINUS' processing; green line: average of PLUS- and MINUS-functions.

In order to calculate an representative shear wave velocity-depth function from line 09SN_13SKEH-M2 at the SED station, all computed 1D-v_S-depth functions between seismic profile station no. 30 and 60 are averaged (non-weighted mean values). The resulting v_S-depth-function is shown in Tab. 3.3b.

Depth [m]	Vs- [m/s]	Vs+ [m/s]	Vs [m/s]
1.0	150	154	152
2.1	155	162	158
3.6	149	118	133
5.5	150	157	153
7.8	188	207	198
10.8	230	252	241
14.4	256	298	264
19.0	309	341	325
24.6	300	365	332
30.8	564	567	566

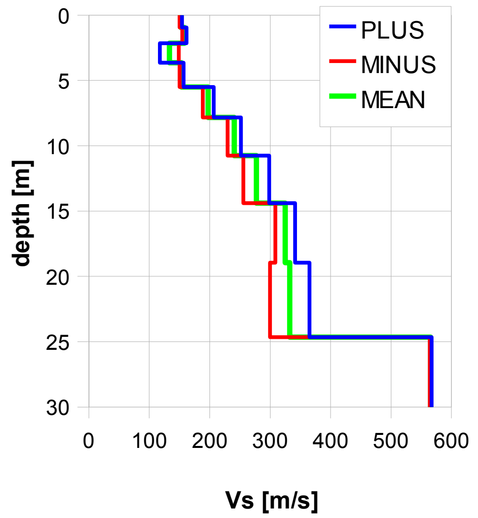

Tab. 3.3b: Averaged v_S - depth function from line 09SN_13SKEH-M2 at the SED station SKEH. Blue line: MASW-'PLUS' processing, red line: MASW-'MINUS' processing; green line: average of PLUS- and MINUS-functions.

The inversion of the four 94 m-array dispersion curves data (10 to 104 m offset, see Fig. 3.3f and 3.3g) are given in Tab. 3.3c. These values are complemented with the values derived from the 40 m-arrays analyses (Tab. 3.3a and 3.3b).

	94 m array							40 m array						
depth	m1+	m1-	m2+	m2-	m1	m2	m	depth	m1	depth	m2	depth	m
2.4	451	323	191	197	387	223	322	0.9	204	1.0	152	1.0	178
5.3	401	326	205	255	363	267	311	2.1	151	2.1	158	2.1	155
9.1	436	716	305	329	576	410	486	3.6	136	3.6	133	3.6	135
13.7	653	538	328	340	595	393	506	5.5	205	5.5	153	5.5	179
19.5	749	516	328	516	632	445	531	7.8	256	7.8	198	7.8	227
26.8	619	1025	480	457	822	702	708	10.7	268	10.8	241	10.7	254
35.8	867	1070	512	562	969	803	816	14.3	322	14.4	277	14.3	300
47.2	1412	988	465	881	1200	465	955	18.8	368	19.0	325	18.9	347
61.3	799	1145	686	924	972	686	876	24.5	434	24.6	332	24.5	383
76.7	1542	1940	1013	1095	1741	1013	1498	30.6	740	30.8	566	30.7	653

Tab. 3.3c: v_S-depth values from the four MASW-derived dispersion curves of both seismic line 09SN_13SKEH-M1 and 09SN_13SKEH-M2 using 94 m-arrays. The dispersion curves are shown in Fig. 3.3f and Fig 3.3g.

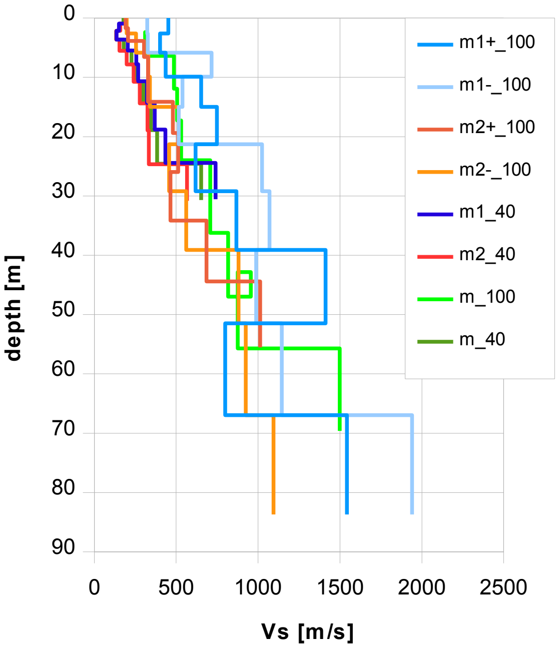

Fig. 3.3j: Comparison of the ensemble of inversion results of both lines 09SN_13SKEH-M1 and -M2, either using the 40 m- and the 94 m-arrays.
blue lines: analyses of records from line 09SN_13SKEH-M1
red lines: analyses of records from line 09SN_13SKEH-M2
violet line: mean of both 94 m-array records analyses in MINUS and PLUS direction.
green lines: v_S-values from analyses of 40 m-array records.

3.3.7 Calculation of the shear wave velocity scalars $v_{s,5}$, $v_{s,10}$, ...

The parameters $v_{s,5}$, $v_{s,10}$, $v_{s,20}$, $v_{s,30}$, $v_{s,40}$, $v_{s,50}$ represent the average shear wave velocities in the depth interval between the surface and the respective depth levels and are determined from the formula

$$v_{s,n} = \frac{\sum_{i=1}^{n} d_i}{\sum_{i=1}^{n} d_i / v_{si}}$$

with:

d_i = thickness of layer i
v_{si} = corresponding shear-wave velocity.

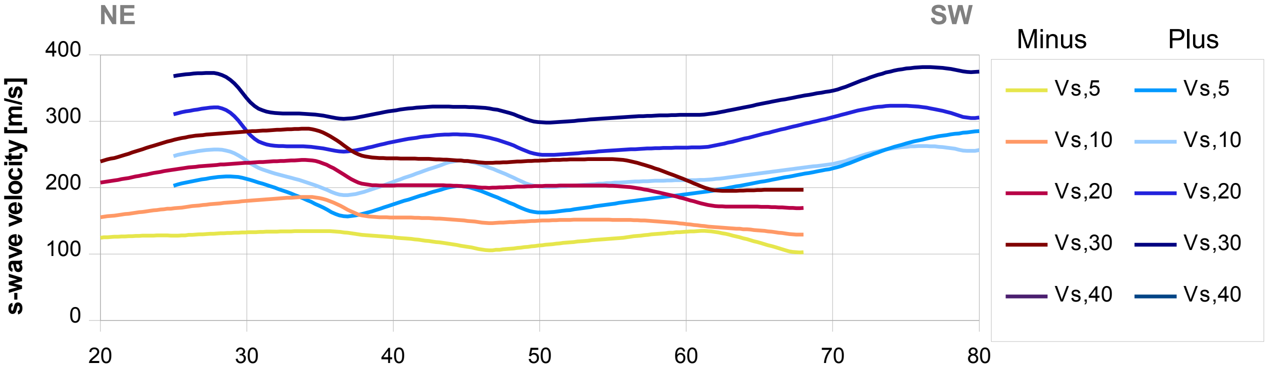

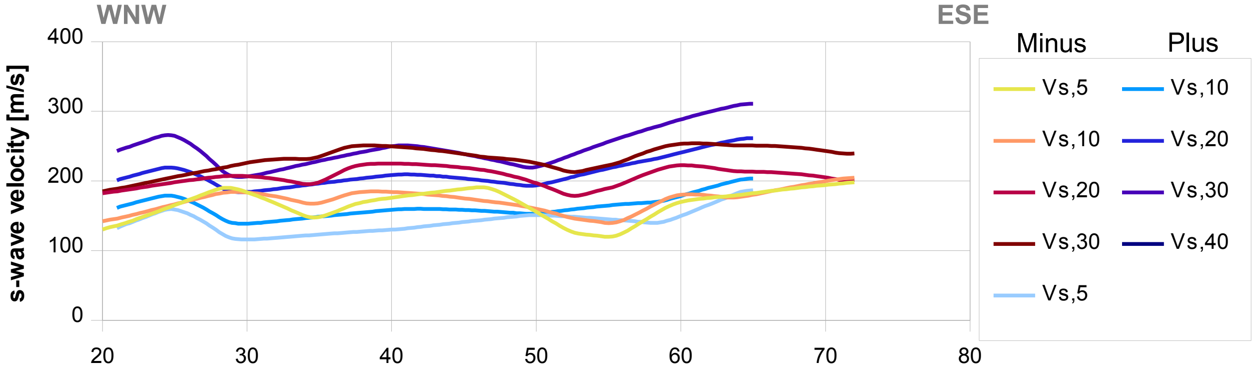

Fig. 3.3k: Graphs of the averaged vs,5...-values along the line 09SN_13SKEH-M1 (top) and -M2 (bottom) for the PLUS- (blue lines) and MINUS- (red lines) directions.

The average values of the s-wave velocity model $v_{s,5}$, $v_{s,10}$, $v_{s,20}$, $v_{s,30}$, $v_{s,40}$, $v_{s,50}$, $v_{s,100}$ (= average shear wave velocity from the surface to depths of 5 m, …until 100 m) on the line segment nearest to the SED station (Tab. 3.3d) are summarized below:

	Vs,5	Vs,10	Vs,20	Vs,30	Vs,40	Vs,50
MINUS	123	159	210	250	n/a	n/a
PLUS	181	213	263	311	n/a	n/a
MEAN	152	186	236	280	n/a	n/a

	Vs,5	Vs,10	Vs,20	Vs,30	Vs,40	Vs,50
MINUS	167	172	206	233	n/a	n/a
PLUS	142	159	206	244	n/a	n/a
MEAN	155	166	206	239	n/a	n/a

Tab. 3.3d: The average shear wave velocities within the depth intervals from surface down to 5 m, etc.… to 50 m, calculated for the line segment with a subjectively most similar geology to the SED station (profile station 30 to 60 for line 09SN_13SKEH-M1, above; profile stations 30 to 60 for line 09SN_16SKEH-M2, below).

3.4 Hybrid Seismic Data Processing

3.4.1 p-wave *Reflection* Seismic Processing Sequence

A) Data conditioning

A1 Reformatting and quality verification of field data
A2 Recording geometry assignment
A3 Data editing (suppression of bad / dead traces, etc.)
A4 Preliminary analysis of refraction velocities

B Filtering and deconvolution

B1 Analytical muting of refraction arrivals
B2 Amplitude recovery / amplitude equalization in time and frequency domains
B3 Predictive deconvolution parameter tests / application
B4 Determination of band limiting corner frequencies / application
B5 Optional 2-D filtering

C) Velocity analysis and stack

C1 Common Depth Point (CDP) sort
C2 Semblance velocity analysis using supergathers of 3 - 5 CDP's
C3 Optional dip move-out correction
C4 Normal Move-Out (NMO) correction and application of stretch mute
C5 Band-pass filtering
C6 CDP stack
C7 Optional coherency filtering

D) Time-depth conversion

D1 Optional spiking deconvolution
D2 Band-pass filtering
D3 Depth conversion
D4 Final display of seismic depth section with inversed polarity (non-SEG-convention)

3.4.2 The presentation of reflection seismic data

The data in a reflection seismic section are presented as an assembly of individual seismic signals at regular intervals along a seismic profile. The simplest way of representing the signals are single wiggle lines (first to the left in the illustration below). A more capturing presentation is the variable area form (second to the left). Combining these two modes results in the var-wiggle mode. Another method of data visualization is the variable density mode (second from the right).

The compressional phase of seismic signals is defined in this report as the onset of the positive amplitude excursion in black (Fig. 3.4a). Since the source signal is produced by an explosion or by an impact at the surface, the signal starts off with a compression of the ground particles. Thus the arrivals of reflection events are defined by the compressional phase.

In rare situations of velocity inversions, cases in which formation velocities are lower than in the layers above, polarity reversals of the reflected signals occur. The beginning of the reflection event would then be characterized by a dilatational phase, represented in this report as a negative amplitude excursion, i.e. in white.

The final p-wave seismic depth sections are displayed in Fig. 3.4b and 3.4c, the hybrid sections in Fig. 3.4j and -k further below.

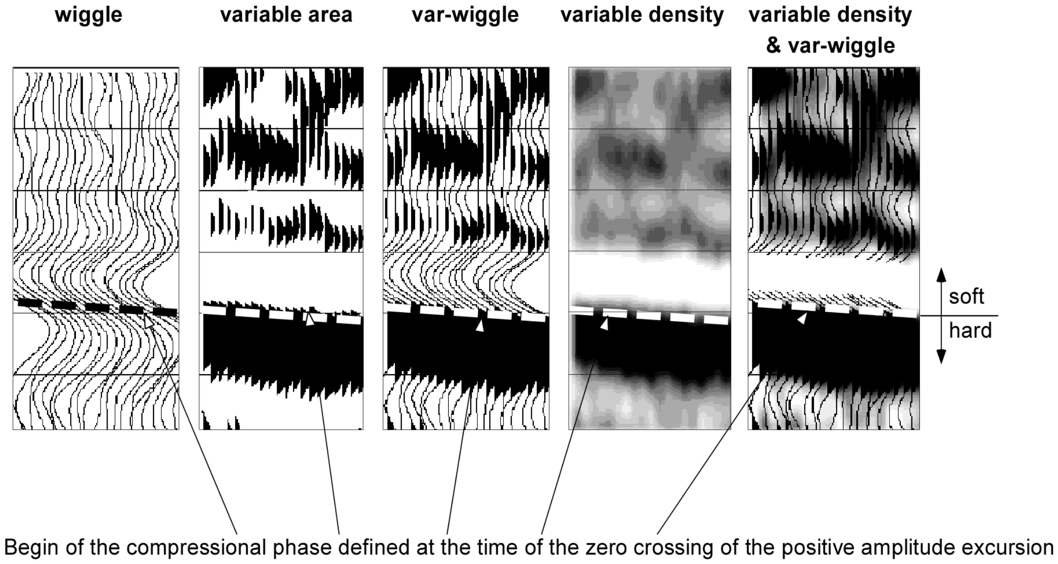

Fig. 3.4a Representation of reflection seismic data and the definition of a reflection event.

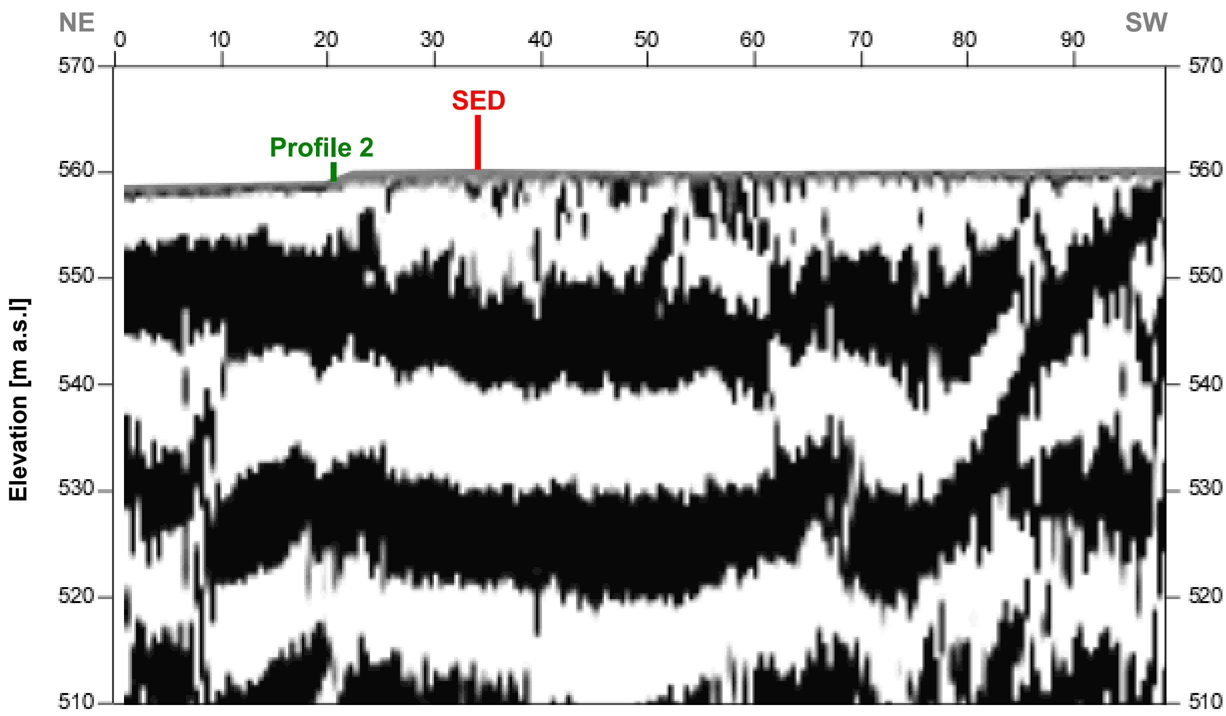

Fig. 3.4b: Seismic depth section of seismic line 09SN_13SKEH-P1 with variable density mode presentation. Vertical axis: elevation [m a.s.l.], horizontal axis: profile meter; no vertical exaggeration. The station spacing is 1 m.

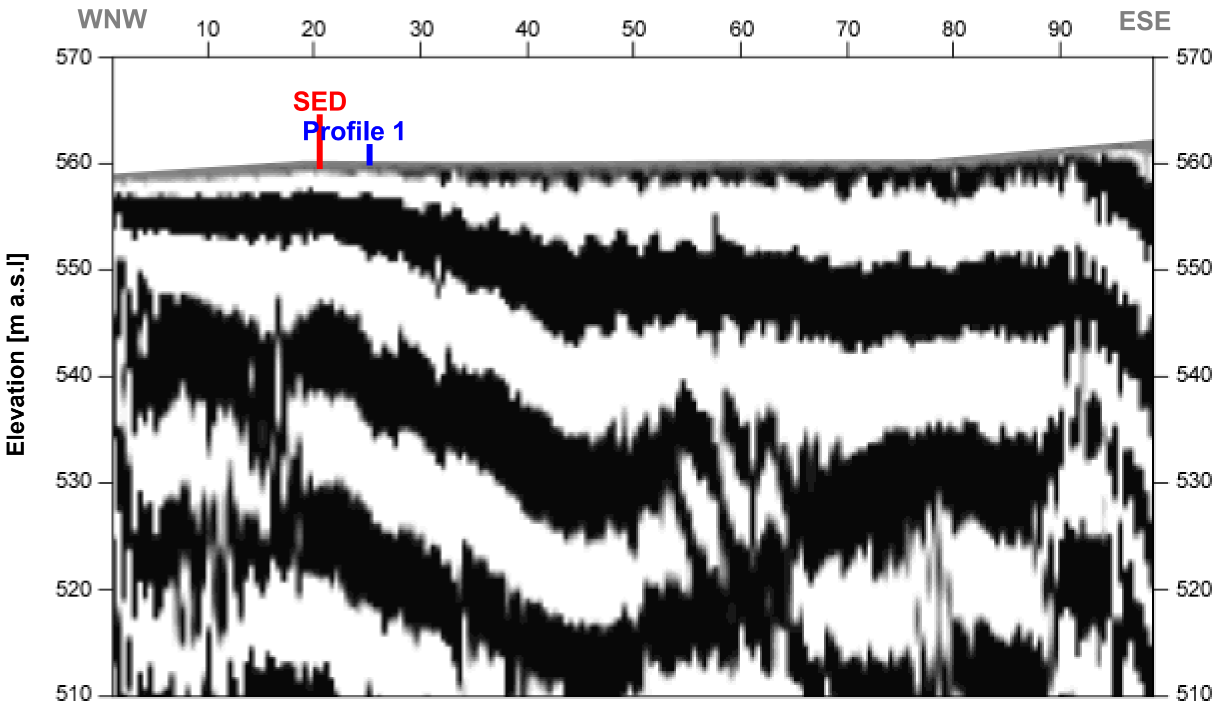

Fig. 3.4c: Seismic depth section of seismic line 09SN_13SKEH-P1 with variable density mode presentation. Vertical axis: elevation [m a.s.l.], horizontal axis: profile meter; no vertical exaggeration. The station spacing is 1 m.

3.4.3 p-wave refraction tomography processing

The seismic p-wave refraction processing steps are analogous to those described in paragraph 3.2. For a detailed method statement and a description of the processing steps please refer to the summary report. The Figs. 3.4d to 3.4i and Tab. 3.4a illustrate the intermediate processing steps and the final result.

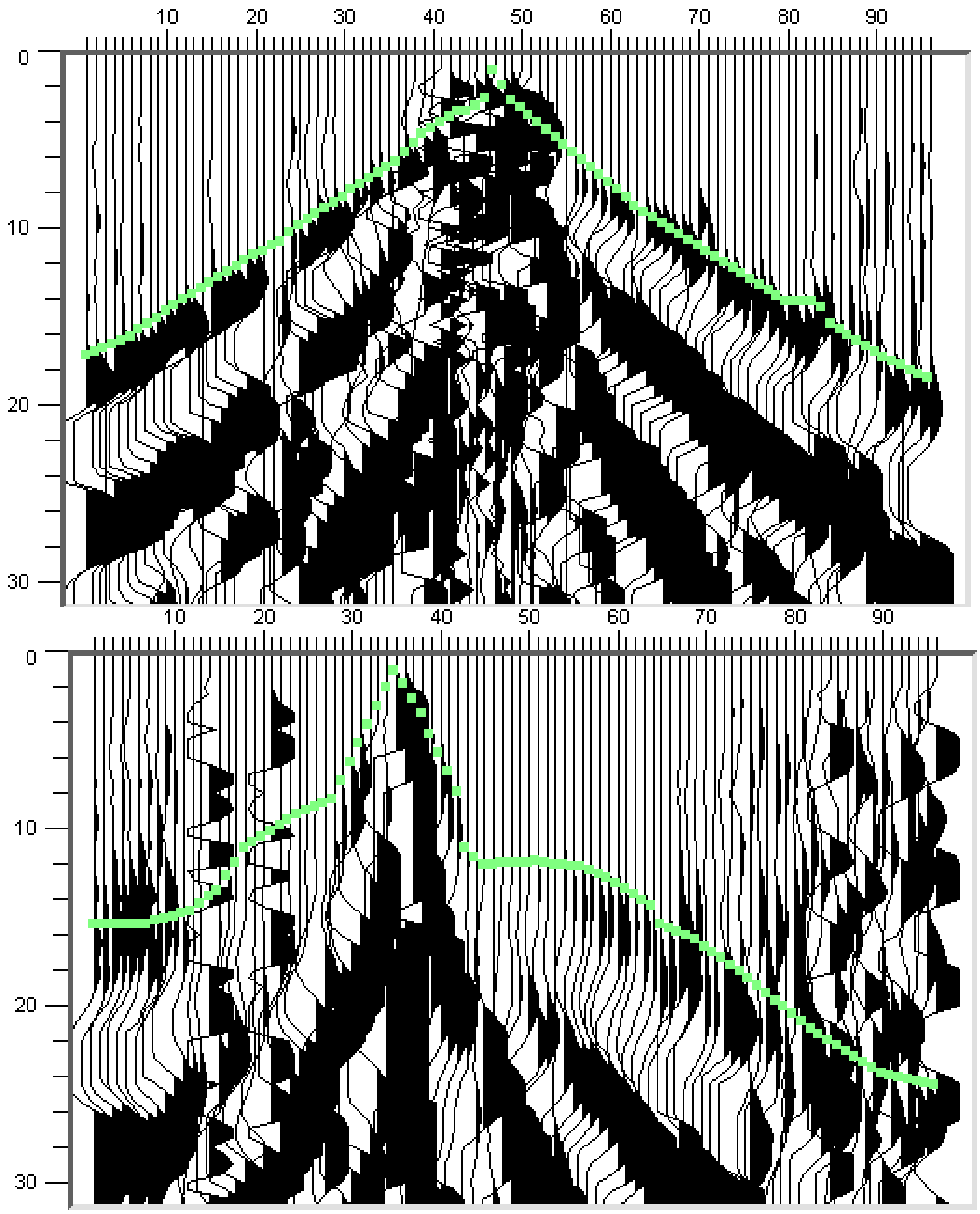

Fig. 3.4d: p-wave records from 09SN_13SKEH-P1 (above) and -P2 (below) with positive amplitude excursions in black. Colored dots mark the manually picked first break arrival times. Vertical axis: travel time in ms, horizontal axis: station numbers spaced at 1 m.

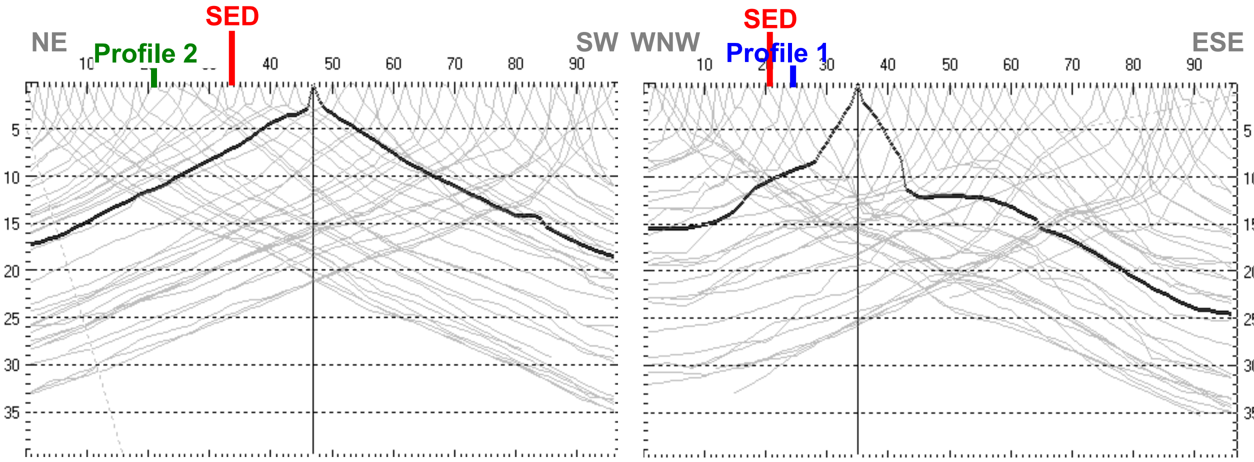

Fig. 3.4e: Travel time curves of p-wave arrival time picks from line 09SN_13SKEH-P1 (left) and -P2 (right). Vertical axes: travel time [ms], horizontal axes: station number (= profile meter).

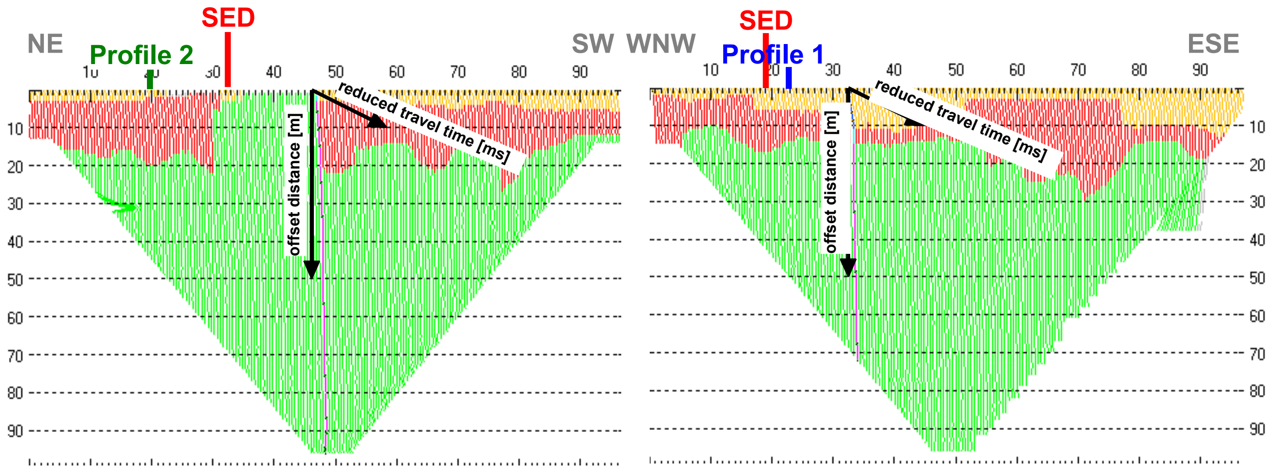

Fig. 3.4f: 3-dimensional distance-travel time diagrams at the mid-points between source points and receiver stations are instrumental when using the analytical CMP derivation of the initial velocity field. The horizontal axes are along the CMP positions and the travel time respectively, the vertical axis denotes the offset distance between source and receiver positions.

Depth [m]	Vs [m/s]
0.2	669
0.5	927
0.8	1137
1.4	1445
2.0	1789
2.9	2088
3.9	2436
5.2	2839
7.1	3423
9.5	3999
12.5	4215
16.4	4523
21.5	4960
28.1	5346
36.7	5344

Depth [m]	Vs [m/s]
0.0	653
0.5	834
0.8	872
1.3	916
2.0	1053
2.8	1393
3.8	2073
5.2	3134
7.0	3595
9.3	3807
12.3	3716
16.2	3689
21.2	3718
27.7	4678
36.2	4685

Tab. 3.4a: Initial 1D p-wave velocity model derived from real data (left: 09SN_13SKEH-P1; right: -P2).

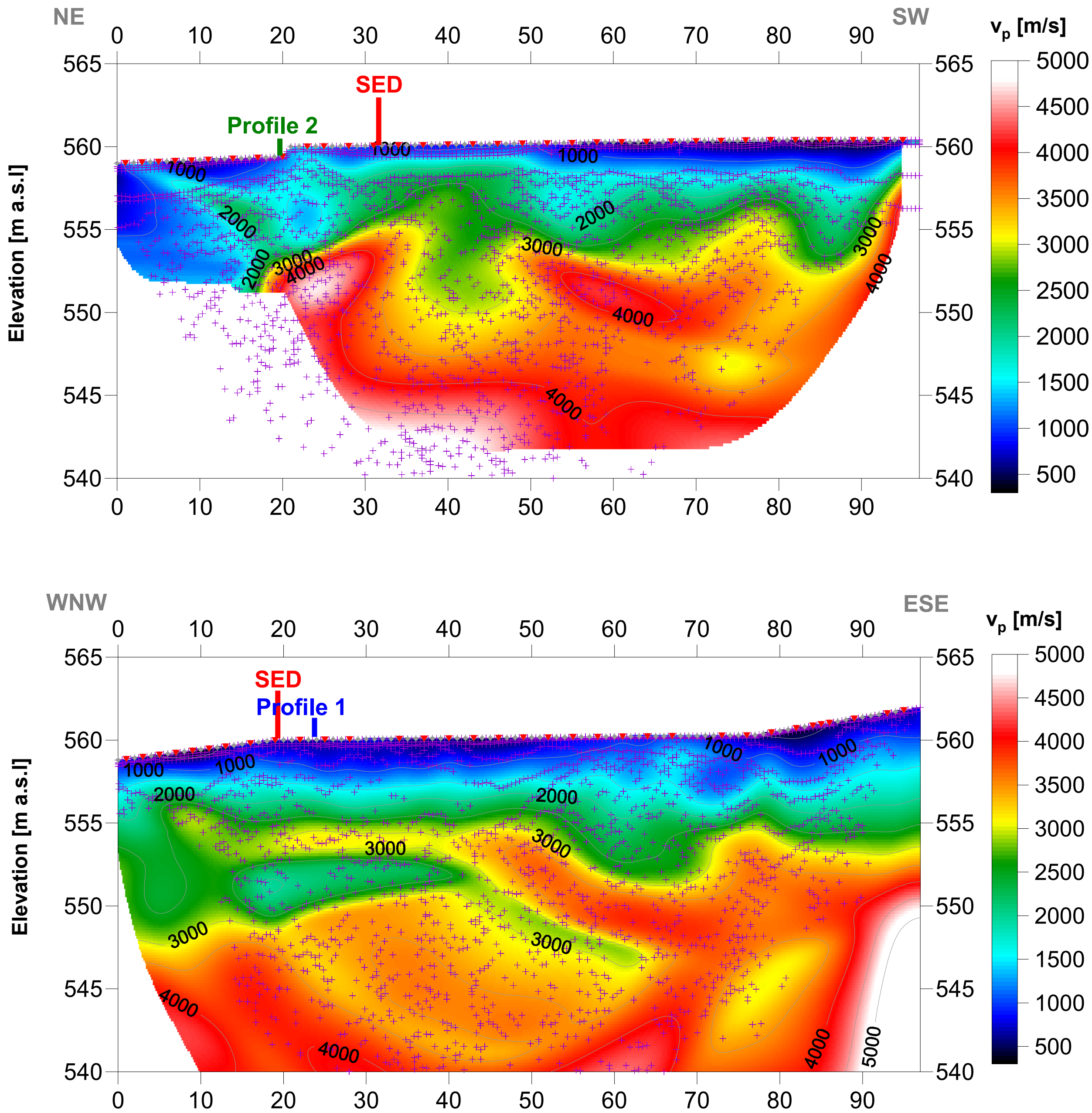

Fig. 3.4g: Compressional wave velocity field image along the seismic profiles 09SN-13SKEH-P1 (top) and -P2 (bottom). Red/white colors indicate solid rock, blue/black colors unconsolidated sediments and soil. Vertical axis: elevation [m a.s.l]; horizontal axis: profile meter; color scale: v_s [m/s]; vertical exaggeration: 2:1; gray squares: receiver stations; red triangles: shot positions; magenta crosses: positions of determined velocity values.

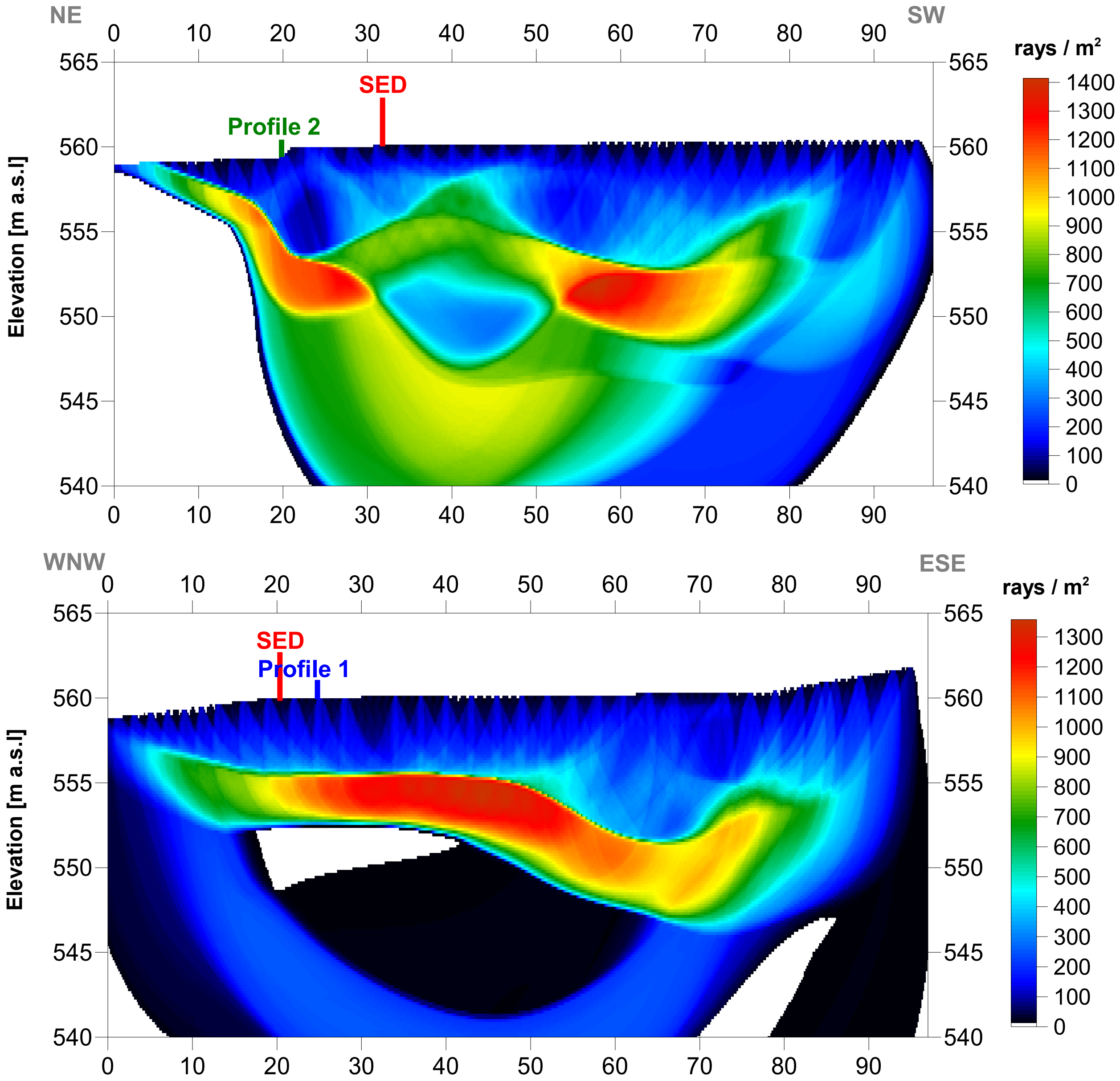

Fig. 3.4h Compressional wave subsurface ray path density along the seismic profiles 09SN_13SKEH-P1 (above) and -P2 (below). Red/white colors indicate high velocity contrast between two layers, blue/black colors low coverage areas. Vertical axis: elevation [m a.s.l]; horizontal axis: profile meter; color scale: ray paths per m2; vertical exaggeration: 2:1.

Depth [m]	Vs [m/s]
0.0	665
1.7	1075
3.3	1809
5.0	2602
6.7	3061
8.3	2935
10.0	3321
11.7	3238
13.3	3293
15.0	3444
16.5	3513
18.2	3554
19.8	3882
21.5	4187
23.2	4192
24.8	3886

Depth [m]	Vs [m/s]
0.0	919
1.5	1810
2.9	2172
4.2	2359
5.6	2756
6.9	3204
8.3	3387
9.6	3346
11.0	3387
12.4	3544
13.7	3800
15.1	4104
16.3	4351
17.6	4493

Tab. 3.4b: Final 1D p-wave velocity model derived from real data at positions most similar to the geological setting at SED station between profile meters 30 and 60 at line 09SN_13SKEH-P1 (left) resp. 30 and 60 at line 09SN_13SKEH-P2 (right) .

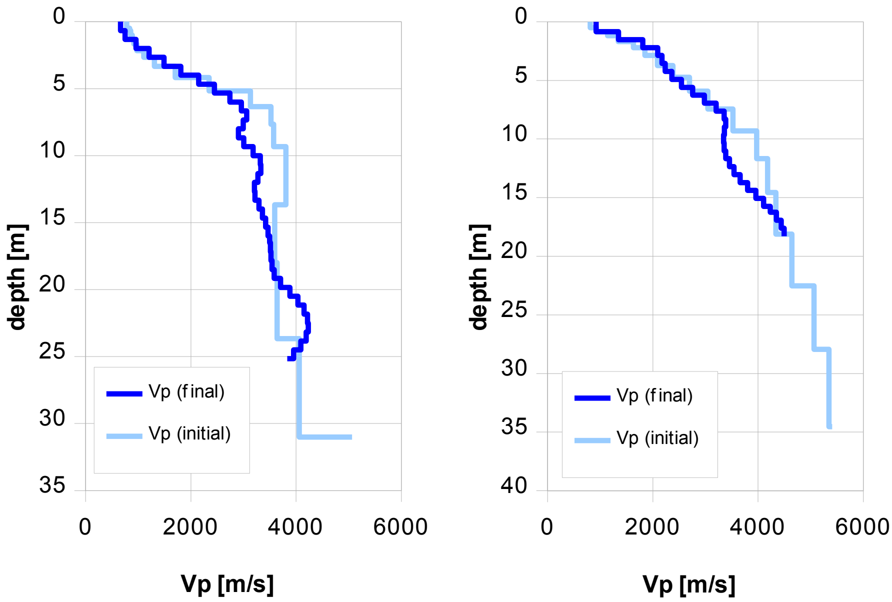

Fig. 3.4i: Final 1D p-wave velocity model derived from real data at a position most similar to the geological setting at the SED station between profile meters 30 and 60 at line 09SN_13SKEH-P1 (left) resp. 30 and 60 at line 09SN_13SKEH-P2 (right). Initial 1D p-wave velocity model values are given in Tab. 3.4a.

3.4.4 Representation of the hybrid seismic section

The hybrid seismic section is the reflection seismic section with the superimposed p-wave velocity field. It portrays the geological structures and the p-wave velocity field, the latter being indicative for the rock / soil rigidity. The uninterpreted hybrid seismic section is portrayed in Fig. 3.4j and 3.4k below.

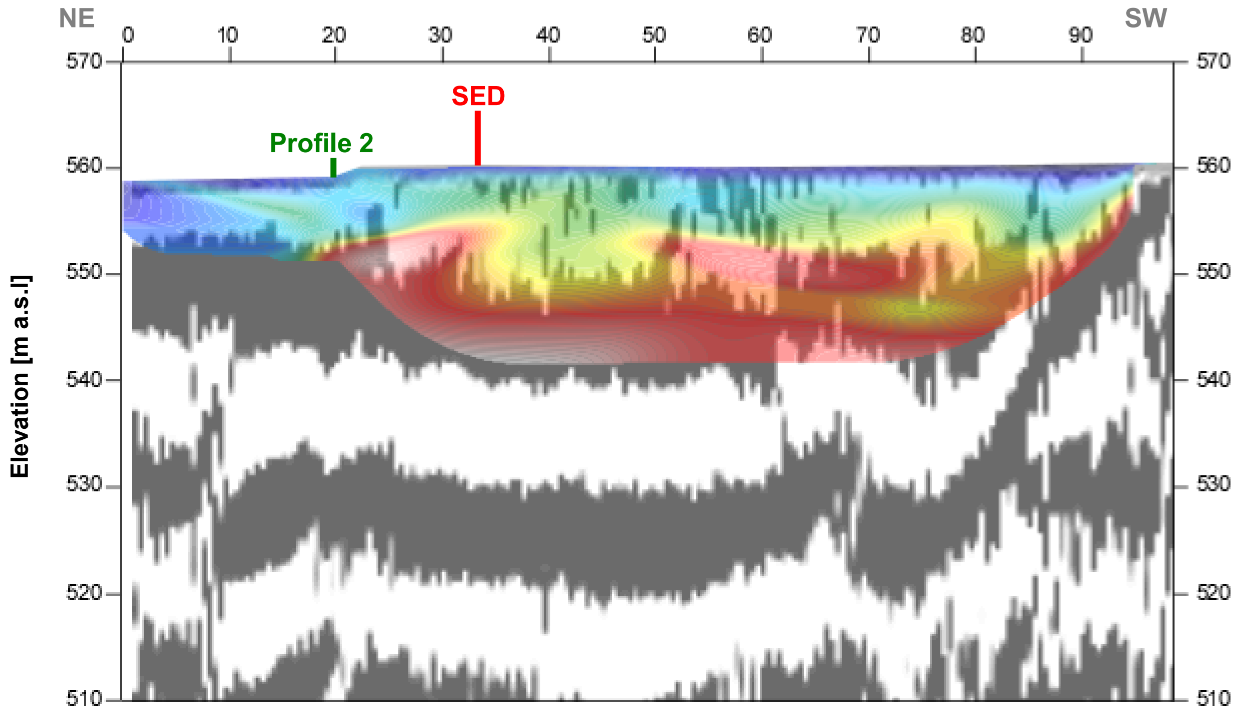

Fig. 3.4j Uninterpreted hybrid seismic section 09SN_13SKEH-P1: superimposed onto the seismic reflection section is the color encoded p-velocity field derived by refraction tomography (no vertical exaggeration).

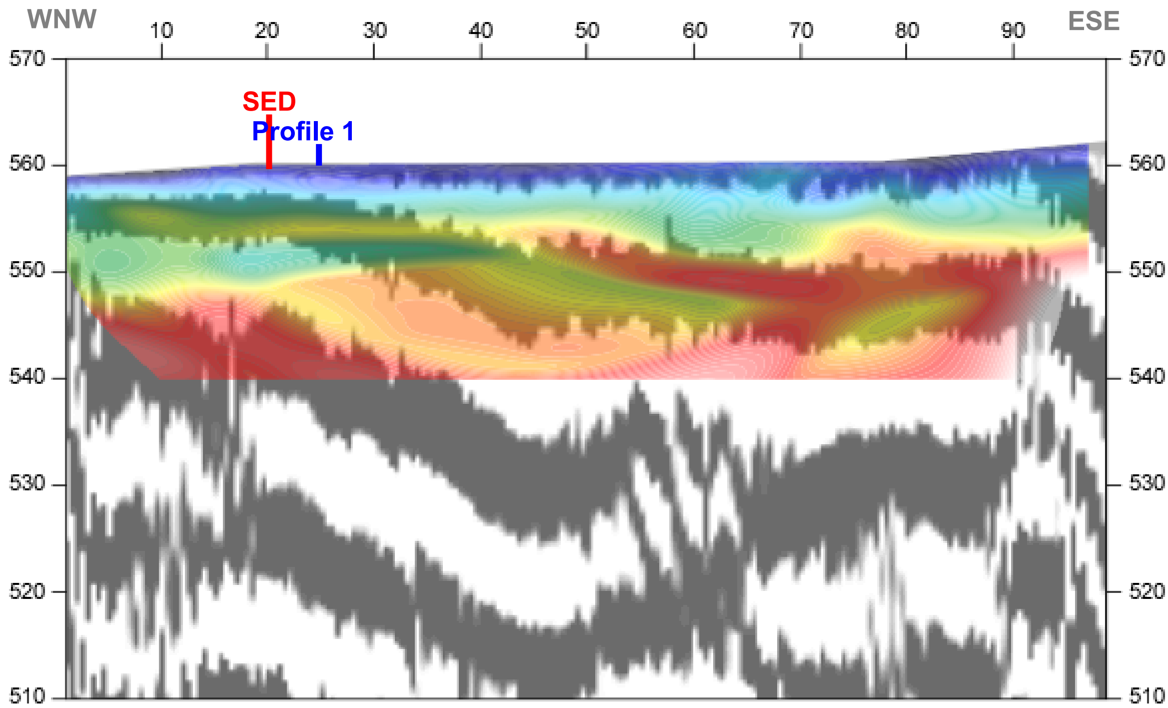

Fig. 3.4k Uninterpreted hybrid seismic section 09SN_13SKEH-P2: superimposed onto the seismic reflection section is the color encoded p-velocity field derived by refraction tomography (no vertical exaggeration).

4 DISCUSSION OF THE RESULTS

4.1 Summary and Validation of the Results

Compressional and shear wave velocity data from refraction seismic surveys both p-wave and s-wave and also the MASW survey data from profiles 09SN_13SKEH-1 and 09SN_13SKEH-2 are shown in Tab. 4.1 for the uppermost 30 m.

Depth	Vp1	Vp2	Vs1	Vs1	Vs2	Vs2	Vs1	Vs2
	meas	meas	meas	calc	meas	calc	MASW	MASW
0	919	665	372	531	184	384		
1	1347	750	387	778	253	433	204	152
2	1810	955	535	1045	423	551	151	158
3	2172	1486	928	1254	774	858	136	133
4	2236	1809	1106	1291	932	1044		
5	2544	2447	1255	1469	1076	1413	205	153
6	2756	2743	1434	1591	1259	1584		
7	3204	3061	1451	1850	1293	1767	256	198
8	3357	2997	1396	1938	1370	1730		
9	3387	3006	1395	1955	1433	1735		
10	3346	3184	1495	1932	1506	1838	268	241
11	3353	3329	1591	1936	1649	1922		
12	3454	3276	1649	1994	1686	1892		
13	3544	3216	1651	2046	1753	1857		
14	3800	3293	1637	2194	1849	1901	322	277
15	3959	3419	1623	2286	1940	1974		
16	4234	3466	1650	2445	2071	2001		
17	4442	3513	1747	2565	2039	2028		
18	4493	3540	1818	2594	1834	2044	368	325
19	4482	3581	1890	2588	1792	2067		
20		3882	2061		1824	2241		
21		4035			1871	2330		
22		4215			1926	2434		
23		4232			2054	2444		
24		4088			2142	2360	434	332
25		3951			2361	2281		
26		3832			2410	2213		
27					2430			
28					2431			
29					2430			
30					2549		740	566

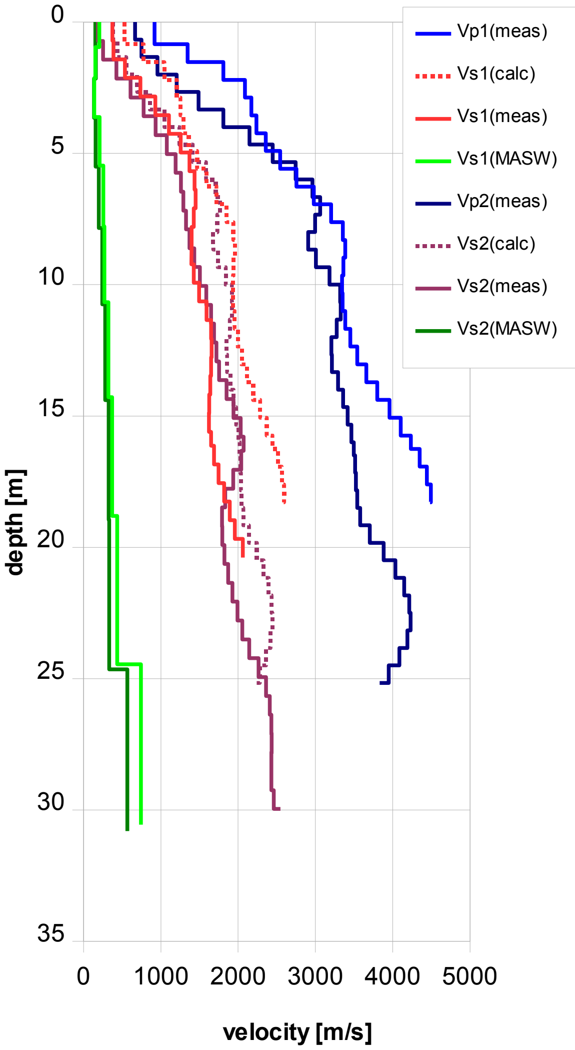

Tab. 4.1: Shear and compressional wave velocity model determined at the SED station SKEH.

Fig. 4.1: Graphic display of shear and compressional wave velocities determined at the SED station. In green colors values from MASW-analyses, in blue values from p-wave refraction tomography and in red from s-wave refraction tomography at the SED station.

4.2 Validation of the methods and their results

Due to methodological differences, v_s velocities derived by MASW analysis and by the refraction tomography technique may differ considerably. This is because MASW analysis cannot image small rock/soil inhomogeneities as a dispersion image with an array length of i.e. 40-m only yields one single v_s-value at each depth. On the other hand, refraction diving wave tomography results produce v_s-sections with a high lateral resolution, but fail to provide information at greater depths.

4.3 Error Estimates

The error estimates given in Tab. 4.3 below are relevant only in the context of this survey.

Surveying method	Type of result	Error estimate
v_S – refraction tomography	v_S – velocity field image	40%
MASW only “+” or only “-“ values	v_S – velocity field image	>100%
MASW (mean of “+” & “-“ values)	v_S – velocity field image	>80%
MASW (94 m array)	v_S – velocity field image	40%
v_P – refraction tomography	v_P – velocity field image	10%
Reflection seismic surveying	Image of subsurface structures	n.a.

Tab. 4.3 Error estimates for the methods applied. Note that higher error estimates are to be taken into account with increasing depths.

The above error estimates are of a qualitative character only. In view of the intense fluctuations to be expected in both the lateral and vertical directions and due to the low quality of data (topography inhomogeneities, 50 Hz interferences, disturbed topmost layers (pavement, buildings) any attempt to derive a quantitative general error estimate to be valid for the entire survey is to be considered as futile.

Due to these high values of estimated errors, the results must be qualified as deficient, explicit the MASW and little less the shear wave refraction values. The calculated ratio of 2 to 6 (depending on depth) between v_S-tomographic and MASW-derivation of the v_S-values and by the relatively good accordance between v_S(measured) and v_S(calculated) (see Tab 4.1) suggest that the MASW-values must be dropped.

At the SED station SKEH (Kerns OW), the refraction velocity images both from shear and compressional wave analysis show related structures. The MASW figures are in the same range as the values obtained from the shear wave diving wave refraction tomography surveys.

4.4 The Geophysical Interpretation

The most conclusive information about the subsurface structures is provided by the results of the hybrid seismic section (v_p-refraction tomography profiling and reflection seismic section) and confirmed by the evaluation results of the v_s-refraction tomography data.

As can be seen from the v_s and v_p refraction tomography sections in Fig. 3.2e/f & Fig. 3.4g/h, the topography of the bedrock surface is imaged rudimentally by high velocity values on both profiles. The geological interpretation of the seismic events is shown in Fig. 4.2a. To the Northeast, it seems that an abundant low velocity layer (debris) is imaged. Bedrock depth is estimated at 5 to 8 m maximum in the central part of the seismic line.

A clearly visible tectonic fault outcrops to the unconsolidated layers at profile meter 60.

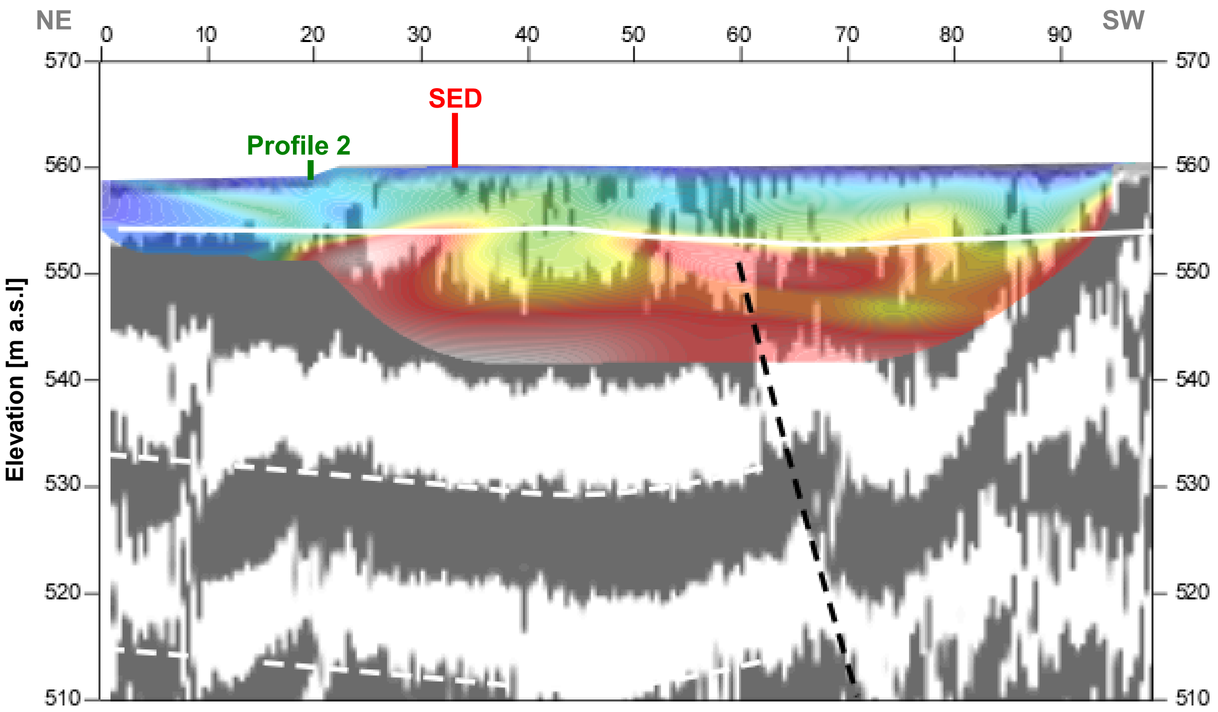

Fig. 4.2a Geophysical interpretation of the hybrid seismic section 09SN_13SKEH-P1. White lines denote layer boundaries, the continuous one the bedrock surface. The steep dipping black dashed line visualizes the assumed tectonic fault.

The geological interpretation of the seismic events of line 09SN_13SKEH-2 is shown in Fig. 4.2b. On the hybrid section 09SN_13SKEH, the topography of the bedrock surface is imaged vaguely all over the profile. The bedrock surface dips from 2 to 10 m depth from WNW to ESE. Like in profile 09SN_13SKEH-1, a tectonic fault is assumed in the middle of the seismic section.

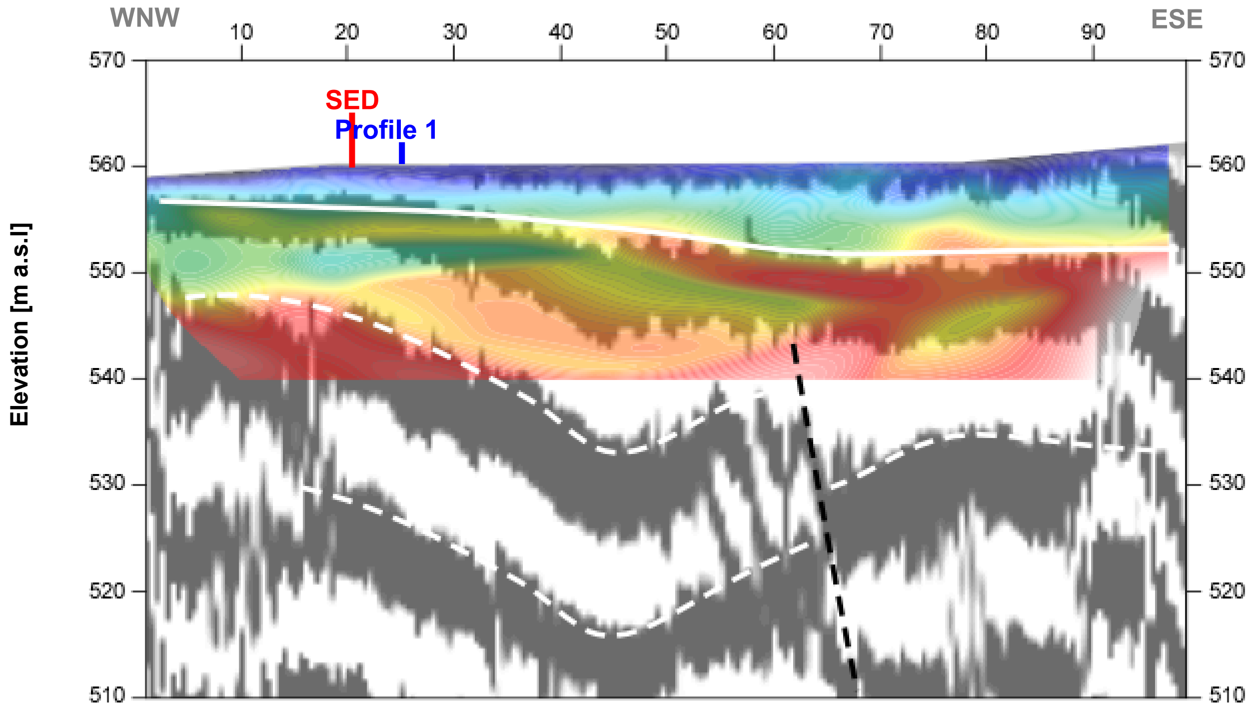

Fig. 4.2b Geophysical interpretation of the hybrid seismic section 09SN_13SKEH-P2. White lines denote layer boundaries, the continuous one marks the bedrock surface; the black dashed line is indicative to a suspected fault.

5 SUMMARY AND CONCLUSIONS

- In March 2009 a combined seismic s- and p-wave survey was carried out at the SED earthquake monitoring station SKEH near Kerns OW.
- The shear wave data have been evaluated by conventional diving wave refraction tomography techniques in order to derive the s-wave velocity field along the seismic line.
- The p-wave data have been processed
  - firstly to derive a 2D s-wave velocity field by using the MASW (**M**ultichannel **A**nalysis of **S**urface **W**aves) technique;
  - and secondly, according to the hybrid seismic data processing scheme for representing the subsurface structures in a combined reflection seismic section with the superimposed p-wave velocity field.
- The shear wave velocity range determined by the MASW method in the uppermost 30 meters spans from values of 133 m/s to 434 m/s. These values seem to be too low by a factor of 2 to 6. We suggest to drop the MASW-values.
- The scalar values derived by the MASW survey at the SED station (seismic line 09SN_13SKEH-M1, profile station 45; seismic line 09SN_13SKEH-M2, profile station 45) are the following:

line 1			line 2		
$v_{s,5}$	=	152 m/s	$v_{s,5}$	=	155 m/s
$v_{s,10}$	=	186 m/s	$v_{s,10}$	=	166 m/s
$v_{s,20}$	=	236 m/s	$v_{s,20}$	=	206 m/s
$v_{s,30}$	=	280 m/s	$v_{s,30}$	=	239 m/s
$v_{s,40}$	=	n/a	$v_{s,40}$	=	n/a

- The maximum refraction shear wave velocity derived is 2549 m/s at a depth of 30 m.
- The scalar values derived by the shear wave refraction tomographic survey at the SED station SED station (seismic line 09SN_13SKEH-S1, profile station 45; seismic line 09SN_13SKEH-S2, profile station 45) are the following:

line 1			line 2		
$v_{s,5}$	=	620 m/s	$v_{s,5}$	=	420 m/s
$v_{s,10}$	=	862 m/s	$v_{s,10}$	=	638 m/s
$v_{s,20}$	=	1137 m/s	$v_{s,20}$	=	941 m/s
$v_{s,30}$	=	n/a	$v_{s,30}$	=	1164 m/s
$v_{s,40}$	=	n/a	$v_{s,40}$	=	n/a

- The maximum p-wave velocity determined is 4493 m/s at a depth of 18 m.
- The geophysical interpretation of the subsurface structures in this report are to be validated and incorporated into a comprehensive appraisal by a geologist familiar with the local geological setting.

Schwerzenbach, 25th May 2009

Walter Frei
dipl. Natw. ETH
managing director

Lorenz Keller
dipl. Natw. ETH
project manager